



Unbridged dimeric platinum (III) complexes : synthesis, characterization, reactivity study and oligomerization  
by David Alan Sartori

A thesis submitted in partial fulfillment of the requirements for the degree of Doctor of Philosophy in Chemistry  
Montana State University  
© Copyright by David Alan Sartori (1998)

Abstract:

PtMe<sub>2</sub>(diimine), where diimine = 2,2'-bipyridyl or 1,10-phenanthroline, oxidized with silver(I) salts in the presence of excess pyridine, forms the dimeric Pt(III) complexes, [Pt<sub>2</sub>Me<sub>4</sub>(bipy)<sub>2</sub>(pyr)<sub>2</sub>]X<sub>2</sub> and [Pt<sub>2</sub>Me<sub>4</sub>(bipy)<sub>2</sub>(pyr)<sub>2</sub>]X<sub>2</sub>, X = NO<sub>3</sub>, CF<sub>3</sub>SO<sub>3</sub>. The mixed diimine dimeric Pt(III) complex was also synthesized. Ferrocenium hexafluorophosphate may also be used as an oxidant. Other oxidants, Ce(IV), NO<sup>+</sup>, and Oxone, were used but did not form the dimeric Pt(III) complexes. Hydrogen peroxide worked to a limited extent.

The dimeric Pt(III) complex, [Pt<sub>2</sub>Me<sub>4</sub>(bipy)<sub>2</sub>(pyr)<sub>2</sub>]X<sub>2</sub>, X = NO<sub>3</sub>, was obtained as a single crystal and the molecular structure was determined by X-ray crystallography. The structure, which contained disordered nitrates and one water per platinum, showed a dimeric Pt(III) complex that was unsupported by bridging ligands. The Pt-Pt metal separation was determined to be 2.708(1) Å.

The reactivity of the newly synthesized dimeric Pt(III) complexes was studied. When axial ligand substitution reactions are performed with triphenylphosphine, the dimeric Pt(III) complexes disproportionated into equimolar fac-[PtIVMe<sub>3</sub>(diimine)(PPh<sub>3</sub>)]<sup>+</sup> and [Pt<sup>III</sup>Me(diimine)(PPh<sub>3</sub>)]<sup>+</sup> complexes. When diimine = phen and in the presence of excess PPh<sub>3</sub>, [Pt<sup>III</sup>Me<sub>2</sub>(phen)(PPh<sub>3</sub>)]<sup>2+</sup> was observed at 243 K. Axial ligand substitution with chloride or thiocyanate formed new, stable complexes. The dimeric complex may be synthesized in the presence of thiocyanate. Evidence of oligomer formation is presented.

A preliminary reactivity study of PtMe<sub>2</sub>(bipy) in the presence of Zn(II), Zr(IV), Cd(II) and Hg(II) salts was performed. Zn(II) and Zr(IV) both formed a Pt-M adduct. Cd(II) formed two different adducts with the Pt complex: Cd-Pt<sub>4</sub> and Cd-Pt. A computer generated structure of the Cd-Pt<sub>4</sub> adduct is presented. Hg(II) forms a Hg-Pt adduct at low equivalents of Hg(II). At one equivalent of Hg(II), two new mercury complexes, [Hg<sup>II</sup>Me(bipy)]<sup>+</sup> and Hg<sub>2</sub>Me(CH<sub>3</sub>CO<sub>2</sub>) are proposed to form. The platinum complex was apparently de-methylated.

An equilibrium study between bis-μ-dialkylsulfidebisdimethylplatinum(II) and free dialkylsulfide to form monomeric cis-bis(dialkylsulfide)dimethyl platinum(II) was performed. The equilibrium constants and thermodynamic parameters of these reactions are reported for methyl, ethyl, and propyl sulfides. Enthalpies and entropies were negative for each reaction and the dimeric complexes owed their existence to an unfavorable entropy value.

UNBRIDGED DIMERIC PLATINUM(III) COMPLEXES: SYNTHESIS,  
CHARACTERIZATION, REACTIVITY STUDY AND OLIGOMERIZATION

by

David Alan Sartori

A thesis submitted in partial fulfillment  
of the requirements for the degree

of

Doctor of Philosophy

in

Chemistry

MONTANA STATE UNIVERSITY-BOZEMAN  
Bozeman, Montana

August 1998

D378  
Sa 776

ii

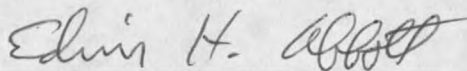
APPROVAL

of a thesis submitted by

David Alan Sartori

This thesis has been read by each member of the thesis committee and has been found to be satisfactory regarding content, English usage, format, citations, bibliographic style, and consistency, and is ready for submission to the College of Graduate Studies.

Edwin H. Abbott



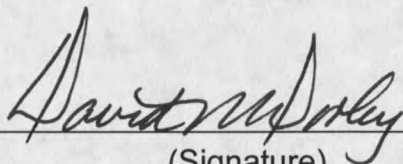
(Signature)

8/12/98

Date

Approved for the Department of Chemistry

David M. Dooley



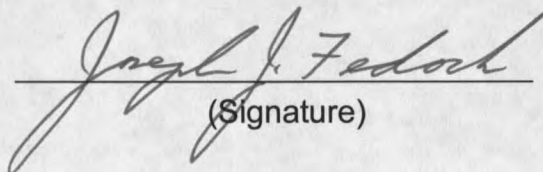
(Signature)

8/12/98

Date

Approved for the College of Graduate Studies

Joseph J. Fedock



(Signature)

8/16/98

Date

## STATEMENT OF PERMISSION OF USE

In presenting this thesis in partial fulfillment of the requirements for a doctoral degree at Montana State University-Bozeman, I agree that the Library shall make it available to borrowers under the rules of the Library. I further agree that copying of this thesis is allowable only for scholarly purposes, consistent with "fair use" as prescribed in the U.S. Copyright Law. Requests for extensive copying or reproduction of this thesis should be referred to University Microfilms International, 300 North Zeeb Road, Ann Arbor, Michigan 48106, to whom I have granted "the exclusive right to reproduce and distribute my dissertation in and from microform along with the non-exclusive right to reproduce my abstract in any format in whole or part."

Signature: Date: 12 August 1998

## TABLE OF CONTENTS

	Page
LIST OF TABLES .....	vi
LIST OF FIGURES .....	ix
ABSTRACT.....	xiii
INTRODUCTION .....	1
Quadruply-Bridged Dimeric Pt(III) Complexes .....	2
Sulfate Bridged Complexes .....	3
Phosphate-Bridged Complexes .....	5
Diphosphite Bridged Complexes.....	7
Acetate and Acetylacetonate Bridged Complexes .....	9
Dithiocarboxylate Bridged Complexes .....	12
Pyrimidine-thionate and Pyridine-thiol Bridged Complexes .....	14
Doubly-Bridged Dimeric Pt(III) Complexes.....	16
$\alpha$ -Pyridone and Pyrimidine Bridged Complexes .....	17
Carboxylate Bridged Complexes .....	20
Hydroxypridinate-Bridged Complexes .....	23
Other Dimeric Pt(III) Complexes .....	29
Unbridged Dimeric Pt(III) Complexes .....	30
Mononuclear Pt(III) Complexes .....	33
EXPERIMENTAL METHODS .....	35
Preparation of Complexes.....	35
Starting Materials.....	35
Tetramethylbis( $\mu$ -diethyl sulfide)diplatinum(II) ( <b>30</b> ) and Tetramethylbis( $\mu$ -dipropyl sulfide)diplatinum(II) ( <b>31</b> ).....	36
Tetramethylbis( $\mu$ -dimethyl sulfide)diplatinum(II) ( <b>32</b> ).....	36
Bipyridyldimethylplatinum(II) ( <b>33</b> ) and Dimethylphenanthrolineplatinum(II) ( <b>34</b> ).....	36
Biquinolinedimethylplatinum(II) ( <b>35</b> ).....	36
Bis(bipyridyl)tetramethylbis(pyridyl)diplatinum(III) dication ( <b>36</b> ) and Tetramethylbis(phenanthroline)bis(pyridyl)diplatinum(III) dication ( <b>37</b> ).....	37
Substitution of axial ligands on <b>36</b> and <b>37</b> .....	38

Mixture of <b>36</b> , <b>37</b> , and Bipyridyltetramethylphenanthrolinebis(pyridyl)- diplatinum(III) dication ( <b>38</b> ) .....	38
Tetramethylbis(phenanthroline)bis(thiocyanato)diplatinum(III) ( <b>39</b> ).....	39
Thermodynamic Study .....	39
Kinetic Analysis .....	40
Methyl Migration Study.....	41
Instrumental Methods.....	41
Nuclear Magnetic Resonance.....	41
Ultraviolet-Visible Spectroscopy .....	42
Electron Paramagnetic Resonance .....	42
 RESULTS AND DISCUSSION .....	 43
Starting Materials: PtMe <sub>2</sub> (bipy) and PtMe <sub>2</sub> (phen).....	43
Reactivity of the PtMe <sub>2</sub> (diimine) complexes.....	44
Crystal Structures of the PtMe <sub>2</sub> (diimine) complexes and derivatives.....	45
Preparation of the Dimeric Pt(III) Complexes .....	69
Preparation of the dimeric Pt(III) species: <b>36</b> and <b>37</b> .....	70
Characterization of the dimeric complexes, <b>36</b> and <b>37</b> .....	84
Preparation and Characterization of Mixed Dimeric Pt(III) Complexes: <b>36</b> , <b>37</b> , and <b>38</b> .....	98
Kinetic Study of Metal-Metal Bond Formation.....	99
Reactivity of the Dimeric Pt(III) Complexes: <b>36</b> , <b>37</b> , and <b>38</b> .....	107
Stability .....	108
Axial ligand substitution reactions.....	108
Oligomer Formation Studies .....	131
Adduct Formation .....	152
Thermodynamic Study of Dimer to Monomer Conversion of bis( $\mu$ - dialkylsulfide)bisdimethylplatinum(II) to <i>cis</i> -bis(dialkylsulfide)- dimethylplatinum(II) .....	167
 SUMMARY AND CONCLUSIONS.....	 183
 REFERENCES .....	 188

## LIST OF TABLES

Table	Page
Table 1. Crystallographic data for PtMe <sub>2</sub> (bipy) ( <b>33</b> ) and PtMe <sub>2</sub> (phen) ( <b>34</b> ).....	48
Table 2. Data collection and structure refinement data for <b>33</b> and <b>34</b> .....	49
Table 3. Atomic Coordinates and equivalent isotropic displacement coefficients for <b>33</b> .....	50
Table 4. Bond lengths (Å) for <b>33</b> .....	50
Table 5. Bond angles (°) for <b>33</b> .....	51
Table 6. Anisotropic displacement coefficients (Å <sup>2</sup> ) for <b>33</b> .....	52
Table 7. Atomic Coordinates and equivalent isotropic displacement coefficients for <b>34</b> .....	53
Table 8. Bond lengths (Å) for <b>34</b> .....	54
Table 9. Bond angles (°) for <b>34</b> .....	55
Table 10. Anisotropic displacement coefficients for <b>34</b> .....	56
Table 11. Crystallographic data for Pt(bipy)Br <sub>2</sub> ( <b>40</b> ) and Pt(bipy) <sub>2</sub> ( <b>41</b> ).....	61
Table 12. Data collection and structure refinement data for <b>40</b> and <b>41</b> .....	62
Table 13. Atomic Coordinates and equivalent isotropic displacement coefficients for <b>40</b> .....	63
Table 14. Bond lengths (Å) for <b>40</b> .....	64
Table 15. Bond angles (°) for <b>40</b> .....	64
Table 16. Anisotropic displacement coefficients for <b>40</b> .....	65
Table 17. Atomic Coordinates and equivalent isotropic displacement coefficients for <b>41</b> .....	66

Table 18. Bond lengths (Å) for <b>41</b> .....	67
Table 19. Bond angles (°) for <b>41</b> .....	67
Table 20. Anisotropic displacement coefficients (Å <sup>2</sup> ) for <b>41</b> .....	68
Table 21. Distances (Å) from the bisecting plane to the designated atoms. ....	89
Table 22. Crystallographic data for bis(bipyridyl)tetramethylbipyridyl- diplatinum(III) dinitrate dihydrate ( <b>36</b> ). ....	92
Table 23. Data collection and structure refinement data for <b>36</b> .....	93
Table 24. Atomic Coordinates and equivalent isotropic displacement coefficients for <b>36</b> .....	94
Table 25. Bond lengths (Å) for <b>36</b> .....	95
Table 26. Bond angles (°) for <b>36</b> .....	96
Table 27. Anisotropic displacement coefficients (Å <sup>2</sup> ) for <b>36</b> .....	97
Table 28. Rate constant dependence, assuming first order, on the concentration of pyridine.....	103
Table 29. Rate constant dependence, assuming first order, of the disappearance of the Pt-Ag adduct on the concentration of added dimeric Pt(III) ([Pt <sup>III</sup> <sub>2</sub> ], <b>36</b> ). ....	106
Table 30. Table listing the chemical shifts ( <sup>1</sup> H only) and <sup>2</sup> J[Pt-H] coupling constants for the species discussed in this dissertation.....	130
Table 31. Integration values for three Pt solutions. The concentration of the trimer was based upon 0.67 unpaired electron equivalents. Calculated values for tetramer (0.50 unpaired electron) and pentamer (0.40 unpaired electron) are also provided. All concentrations are mM. ....	135
Table 32. Absorption data for the Jobs study of the trimer solution of <b>33</b> and <b>36</b> . λ <sub>350</sub> is λ <sub>max</sub> for <b>36</b> and λ <sub>456</sub> is λ <sub>max</sub> for <b>33</b> . Across the top of the table are the volumes ( <b>33:36</b> ) of each 0.250 mM solution in mL.....	138



Table 33. Beer's Law absorbance data for <b>33</b> and <b>36</b> at the concentrations studied. ....	142
Table 34. List of $\epsilon$ values calculated at 310, 350, 456, 480 and 500 nm by linear regression plots for <b>33</b> and <b>36</b> . R values were 0.99. ....	145
Table 35. Bond lengths ( $\text{\AA}$ ) of Pt-Cd, Pt-N(bipy), and Pt-C(Me) of the Pt <sub>4</sub> -Cd adduct and of complexes <b>33</b> , <b>34</b> and <b>36</b> . See numbering schemes of Figures 1, 2 and 18. ....	161
Table 36. Equilibrium values ( $M^{-1}$ ) for each equivalent of SR <sub>2</sub> (R = Me, Et and Pr) at 303.2 K. ....	172
Table 37. Equilibrium constants at 303 K and thermodynamic parameters for the reaction $[\text{Pt}_2\text{Me}_4(\mu\text{-SR}_2)_2] + 2 \text{SR}_2 \rightleftharpoons 2 \text{cis-}[\text{PtMe}_2(\text{SR}_2)_2]$ . ....	173
Table 38. Crystallographic data for <i>trans</i> -dichlorobis(dibenzylsulfide) platinum(II) ( <b>42</b> ). ....	177
Table 39. Data collection and structure refinement data for <b>42</b> . ....	178
Table 40. Atomic Coordinates and equivalent isotropic displacement coefficients for <b>42</b> . ....	179
Table 41. Bond lengths ( $\text{\AA}$ ) for <b>42</b> . ....	180
Table 42. Bond angles ( $^\circ$ ) for <b>42</b> . ....	181
Table 43. Anisotropic displacement coefficients ( $\text{\AA}^2$ ) for <b>42</b> . ....	182

## LIST OF FIGURES

Figure	Page
Figure 1. Thermal ellipsoid plot of <b>33</b> .....	46
Figure 2. Thermal ellipsoid plot of <b>34</b> .....	47
Figure 3. Thermal ellipsoid plot of <b>40</b> .....	59
Figure 4. Thermal ellipsoid plot of <b>41</b> .....	60
Figure 5. $^1\text{H}$ NMR spectrum of decomposition products from the reaction of <b>33</b> with silver(I) in acetonitrile- $\text{d}_3$ .....	71
Figure 6. $^1\text{H}$ NMR spectrum of decomposition products from the reaction of <b>34</b> with silver(I) in acetonitrile- $\text{d}_3$ .....	72
Figure 7. First appearance of the dimeric Pt(III) complex, <b>36</b> .....	74
Figure 8. Stacked plot showing the disappearance of the Pt-Ag adduct peak and the appearance of the new species over a period of 30 minutes.....	76
Figure 9. Decomposition of the dimeric Pt(III) complex in the presence of only one equivalent of pyridine.....	77
Figure 10. $^1\text{H}$ NMR spectrum of pure <b>36</b> obtained after removing the solvent under high vacuum.....	79
Figure 11. $^1\text{H}$ NMR spectrum of the result of oxidizing <b>33</b> with Ce(IV).....	80
Figure 12. $^1\text{H}$ NMR spectrum of the result of oxidizing <b>33</b> with $\text{NO}^+$ .....	81
Figure 13. $^1\text{H}$ NMR spectrum of the result of oxidizing <b>33</b> with Oxone.....	82
Figure 14. $^1\text{H}$ NMR spectrum of the result of oxidizing <b>33</b> with hydrogen peroxide.....	83
Figure 15. $^1\text{H}$ NMR spectrum of <b>37</b> in the presence of excess pyridine.....	85

Figure 16. $^{13}\text{C}$ NMR spectrum of complex <b>36</b> only showing the Me-Pt region. .	86
Figure 17. $^{13}\text{C}$ NMR spectrum of complex <b>37</b> only showing the Me-Pt region. .	87
Figure 18. Thermal ellipsoid plot of the dication <b>36</b> .....	90
Figure 19. Perspective view down the Pt-Pt bond of <b>36</b> .....	91
Figure 20. $^1\text{H}$ NMR spectrum showing the 1:2:1 distribution of complexes <b>37</b> , <b>38</b> , and <b>36</b> .....	100
Figure 21. First order rate plots for the pyridine analyses.....	102
Figure 22. A stacked plot of first order plots of the five dimeric Pt(III) ( <b>36</b> ) concentration studies on the rate of the reaction. 10 $\mu\text{L}$ = 0.556 mM, 30 $\mu\text{L}$ = 1.65 mM, 50 $\mu\text{L}$ = 2.71 mM, 70 $\mu\text{L}$ = 3.75 mM and 100 $\mu\text{L}$ = 5.25 mM.....	106
Figure 23. Appearance of the $\text{Pt}^{\text{IV}}\text{Me}_3(\text{pyr})$ peak from the disproportionation species $\text{Pt}^{\text{IV}}\text{Me}_3(\text{PPh}_3)$ .....	111
Figure 24. An offset stacked plot showing the slow equilibrium of formation of $\text{Pt}^{\text{IV}}\text{Me}_3(\text{PPh}_3)$ from $\text{Pt}^{\text{IV}}\text{Me}_3(\text{pyr})$ .....	112
Figure 25. A stacked plot of the Me-Pt region showing the peak shift from pure <b>37</b> to the new peak formed upon addition of $\text{PPh}_3$ .....	114
Figure 26. Low temperature study of the formation of the bis-axial phosphine complex of <b>37</b> .....	115
Figure 27. The equilibrium distribution of <b>37</b> , <b>38</b> and <b>36</b> after the addition of approximately 0.5 equivalents of $\text{PPh}_3$ . ....	117
Figure 28. Me-Pt region of the reaction of the mixed dimeric Pt(III) complexes with 0.5 equivalents $\text{PPh}_3$ . ....	118
Figure 29. The addition of 0.75 equivalents of $\text{PPh}_3$ to a solution containing <b>37</b> , <b>38</b> and <b>36</b> . ....	119
Figure 30. Me-Pt region of the 0.75 equivalent $\text{PPh}_3$ reaction. ....	120
Figure 31. $^1\text{H}$ NMR spectrum of the reaction of <b>36</b> with excess $\text{SCN}^-$ .....	124
Figure 32. $^1\text{H}$ NMR spectrum of the reaction of <b>37</b> with excess $\text{SCN}^-$ .....	125

Figure 33. The reaction of <b>34</b> in the presence of $\text{SCN}^-$ with silver(I). .....	126
Figure 34. Polymer of $[\text{Ag}(\text{SCN})]_n$ that was formed (85). .....	127
Figure 35. Chloride axial substitution of <b>36</b> . .....	128
Figure 36. Chloride axial substitution of <b>37</b> . .....	129
Figure 37. $^1\text{H}$ NMR spectrum of the trimer solution prepared from <b>33</b> and <b>36</b> . .....	132
Figure 38. EPR spectrum of the trimer solution prepared from <b>33</b> and <b>36</b> . .....	133
Figure 39. EPR spectrum of the trimer solution prepared from <b>34</b> and <b>37</b> . .....	134
Figure 40. The absorption spectra from the Jobs plot performed on the trimer ratio of <b>33</b> and <b>36</b> . .....	139
Figure 41. The Beer's Law study of <b>33</b> . .....	140
Figure 42. The Beer's Law study of <b>36</b> . .....	141
Figure 43. Absorbance vs. concentration linear regression plots for <b>33</b> at 310, 350, 456, 480 and 500 nm. .....	143
Figure 44. Absorbance vs. concentration linear regression plots for <b>36</b> at 310, 350, 456, 480 and 500 nm. .....	144
Figure 45. Disproportionation species obtained from reacting one mole of <b>33</b> with one mole of <b>36</b> . .....	146
Figure 46. Disproportionation species obtained from reacting one mole of <b>34</b> with one mole of <b>37</b> . .....	147
Figure 47. Disproportionation species of the reaction of one mole <b>33</b> with one mole <b>37</b> . .....	148
Figure 48. Disproportionation species of the reaction of one mole <b>34</b> with one mole <b>36</b> . .....	149
Figure 49. Stacked plot of (a) a mixture of <b>33</b> (1) and <b>34</b> (2), (b) the mixed dimeric Pt(III) complexes, <b>37</b> (3), <b>38</b> (4) and <b>36</b> (5) and (c) the trimer mixture of <b>36</b> and <b>34</b> . .....	150
Figure 50. The $\text{Pt}_2\text{-Ag}$ adduct that Puddephatt characterized (79). .....	153

Figure 51. Proposed structure of the Pt-Ag adduct (79).....	153
Figure 52. $^1\text{H}$ NMR (300 MHz) spectrum of the adduct Pt-Zr.....	155
Figure 53. $^1\text{H}$ NMR (300 MHz) spectrum of the adduct Pt-Zn.....	156
Figure 54. $^1\text{H}$ NMR (300 MHz) stacked plot of the titration of <b>33</b> with Cd(II) showing the Me-Pt region. ....	158
Figure 55. $^1\text{H}$ NMR (300 MHz) stacked plot of the titration of <b>33</b> with Cd(II) showing the aromatic region. ....	159
Figure 56. MacSpartan Plus <sup>®</sup> model of the Pt <sub>4</sub> -Cd adduct.....	160
Figure 57. $^1\text{H}$ NMR (300 MHz) stacked plot of the titration of <b>33</b> with Hg(II) showing the Me-Pt region. ....	163
Figure 58. $^1\text{H}$ NMR (300 MHz) stacked plot of the titration of <b>33</b> with Cd(II) showing the aromatic region. ....	164
Figure 59. Structure of [Hg(bipy)Me](NO <sub>3</sub> ) (99). ....	165
Figure 60. Proposed structure of species 2, Hg <sub>2</sub> (CH <sub>3</sub> CO <sub>2</sub> )CH <sub>3</sub> .....	166
Figure 61. A $^1\text{H}$ NMR spectrum of <b>32</b> with 1 equivalent of SR <sub>2</sub> = Me.....	168
Figure 62. A $^1\text{H}$ NMR spectrum of <b>30</b> with 1 equivalent of SR <sub>2</sub> = Et. ....	169
Figure 63. A $^1\text{H}$ NMR spectrum of <b>31</b> with 1 equivalent of SR <sub>2</sub> = Pr. ....	170
Figure 64. Thermal ellipsoid plot of <b>42</b> .....	176

## ABSTRACT

$\text{PtMe}_2(\text{diimine})$ , where diimine = 2,2'-bipyridyl or 1,10-phenanthroline, oxidized with silver(I) salts in the presence of excess pyridine, forms the dimeric Pt(III) complexes,  $[\text{Pt}_2\text{Me}_4(\text{bipy})_2(\text{pyr})_2]\text{X}_2$  and  $[\text{Pt}_2\text{Me}_4(\text{bipy})_2(\text{pyr})_2]\text{X}_2$ ,  $\text{X} = \text{NO}_3$ ,  $\text{CF}_3\text{SO}_3$ . The mixed diimine dimeric Pt(III) complex was also synthesized. Ferrocenium hexafluorophosphate may also be used as an oxidant. Other oxidants,  $\text{Ce(IV)}$ ,  $\text{NO}^+$ , and Oxone, were used but did not form the dimeric Pt(III) complexes. Hydrogen peroxide worked to a limited extent.

The dimeric Pt(III) complex,  $[\text{Pt}_2\text{Me}_4(\text{bipy})_2(\text{pyr})_2]\text{X}_2$ ,  $\text{X} = \text{NO}_3$ , was obtained as a single crystal and the molecular structure was determined by X-ray crystallography. The structure, which contained disordered nitrates and one water per platinum, showed a dimeric Pt(III) complex that was unsupported by bridging ligands. The Pt-Pt metal separation was determined to be 2.708(1) Å.

The reactivity of the newly synthesized dimeric Pt(III) complexes was studied. When axial ligand substitution reactions are performed with triphenylphosphine, the dimeric Pt(III) complexes disproportionated into equimolar *fac*- $[\text{Pt}^{\text{IV}}\text{Me}_3(\text{diimine})(\text{PPh}_3)]^+$  and  $[\text{Pt}^{\text{II}}\text{Me}(\text{diimine})(\text{PPh}_3)]^+$  complexes. When diimine = phen and in the presence of excess  $\text{PPh}_3$ ,  $[\text{Pt}^{\text{III}}\text{Me}_2(\text{phen})(\text{PPh}_3)]_2^{2+}$  was observed at 243 K. Axial ligand substitution with chloride or thiocyanate formed new, stable complexes. The dimeric complex may be synthesized in the presence of thiocyanate. Evidence of oligomer formation is presented.

A preliminary reactivity study of  $\text{PtMe}_2(\text{bipy})$  in the presence of  $\text{Zn(II)}$ ,  $\text{Zr(IV)}$ ,  $\text{Cd(II)}$  and  $\text{Hg(II)}$  salts was performed.  $\text{Zn(II)}$  and  $\text{Zr(IV)}$  both formed a Pt-M adduct.  $\text{Cd(II)}$  formed two different adducts with the Pt complex:  $\text{Cd-Pt}_4$  and  $\text{Cd-Pt}$ . A computer generated structure of the  $\text{Cd-Pt}_4$  adduct is presented.  $\text{Hg(II)}$  forms a Hg-Pt adduct at low equivalents of  $\text{Hg(II)}$ . At one equivalent of  $\text{Hg(II)}$ , two new mercury complexes,  $[\text{Hg}^{\text{II}}\text{Me}(\text{bipy})]^+$  and  $\text{Hg}_2\text{Me}(\text{CH}_3\text{CO}_2)$  are proposed to form. The platinum complex was apparently de-methylated.

An equilibrium study between bis- $\mu$ -dialkylsulfidebisdimethylplatinum(II) and free dialkylsulfide to form monomeric *cis*-bis(dialkylsulfide)dimethyl platinum(II) was performed. The equilibrium constants and thermodynamic parameters of these reactions are reported for methyl, ethyl, and propyl sulfides. Enthalpies and entropies were negative for each reaction and the dimeric complexes owed their existence to an unfavorable entropy value.

## INTRODUCTION

One-dimensional materials are the objects of intense study due to their spectacular and highly anisotropic electrical, magnetic and optical properties. Most 1-D electrical conductor platinum complexes contain an infinite stack of planar molecules having platinum atoms of non-integral oxidation number. A major stumbling block that scientists face in searching for strategies to synthesize stacked planar complexes are the complexes' unpredictable packing forces. Scientists wish to devise a synthetic method, which controls the interplay between electronic and packing forces. Consequently, the scientific community must first study these forces in new low-dimensional systems and determine how these factors effect solid-state properties. This thesis outlines the synthetic strategy and characterization of three new unbridged dimeric Pt(III) complexes.

Dimeric  $d^7-d^7$  metal complexes have a net single bond between the metal atoms and possess a  $\sigma^2\pi^4\delta^2\delta^*2\pi^*4$  electronic configuration (1). Typically, these systems have either two or four ligands bridging the two metal centers and have axial ligand positions occupied by suitable monodentate donor ligands. This type of bonding and these types of ligand configurations are commonly seen in  $Rh_2^{4+}$  systems, where numerous examples have been structurally characterized. In comparison to the  $Rh_2^{4+}$  systems, however, the isoelectronic  $Pt_2^{6+}$  systems have only recently been studied, and relatively few examples have been structurally

characterized. Furthermore, only in the last decade have examples of the  $\text{Pt}_2^{6+}$  system been characterized in which there do not exist bridging ligands between the two metal centers. Although this thesis project deals with examples of unbridged  $\text{Pt}_2^{6+}$  systems, a historical background covering both bridged and unbridged systems will be presented.

### Quadruply-Bridged Dimeric Pt(III) Complexes

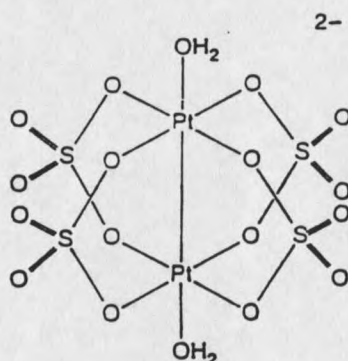
Quadruply-bridged dimeric complexes, also called lantern-type complexes, are observed for a large variety of transition metal ions, e.g., Cu, Cr, Mo, W, Tc, Re, Ru, Os, Rh, Ir, Ni, Pd, and Pt. Complexes containing four bridging ligands appear to be one of the most important common basic structures for transition metal complexes (1-3). However, platinum complexes of this type have been one of the last to be characterized but appear to be the most versatile in regards to the coordinating atoms of the bridging ligands, including O, P, S, C, and N. These bridging ligands commonly form a five-membered ring between the two metal ions. Furthermore, well-characterized lantern-type platinum complexes have been shown to form between divalent, trivalent, and mixed-valent platinum ions.



### Sulfate Bridged Complexes

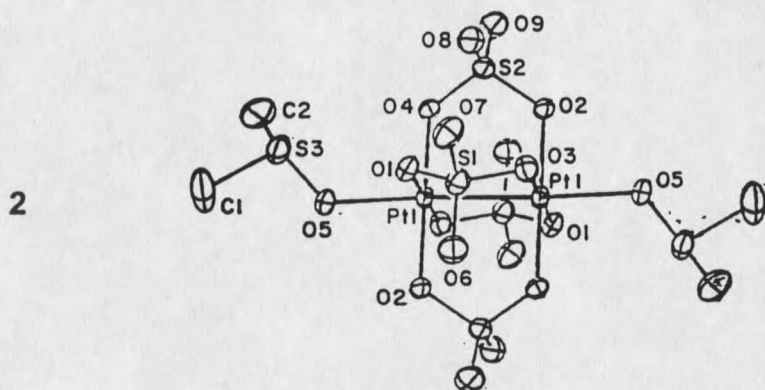
The first dimeric platinum(III) complex was prepared in 1905 by Blondel (4). In a complex reaction in which platinum(IV) oxide was reacted with a sulfuric acid-water mixture that was subsequently reduced by the addition of oxalic acid he formed the dimeric platinum(III) complex,  $\text{H}_2[\text{Pt}_2(\text{SO}_4)_4(\text{H}_2\text{O})_2] \cdot 9.5 \text{H}_2\text{O}$ . Blondel also reported the syntheses of the sodium and potassium salts of this complex (4). Independent confirmation of Blondel's work came several years later when Wöhler and Frey (5) and Delepine (6) developed better methods to prepare his complexes, as well as several other closely related ones. Blondel's work is especially significant in that the potassium salt of his complex,  $\text{K}_2[\text{Pt}_2(\text{SO}_4)_4(\text{H}_2\text{O})_2]$ , would prove to be the first structurally characterized dimeric platinum(III) complex. The complex was prepared by an improved method involving a complex oxidation-reduction reaction between  $\text{K}_2[\text{Pt}(\text{NO}_2)_4]$  and sulfuric acid (7). Soon after this report came an incomplete crystal structure determination in which only average bond lengths and bond angles were reported, with no mention of error estimates (8). Although incomplete, this structure determination showed the anion to have the same type of sulfato-bridged, metal-metal bonded dimeric structure, **1**, seen previously for  $[\text{Re}_2(\text{SO}_4)_4(\text{H}_2\text{O})_2]^{4-}$  (9) and  $[\text{Mo}_2(\text{SO}_4)_4(\text{H}_2\text{O})_2]$  (6-10).

1



The reported Pt-Pt distance of 2.466 Å was consistent with having the  $\sigma^2\pi^4\delta^2\delta^*2\pi^*4$  electronic configuration and a net single bond between the two platinum(III) atoms. In 1984, a complete structure determination that confirmed the earlier results was reported (11). Potentiometric titration with Ti(III) and Cr<sub>2</sub>O<sub>7</sub><sup>2-</sup> provided confirmation of an average platinum oxidation state of +3 (7). X-ray photoelectron spectroscopy (XPS) studies also showed that the two platinum atoms were equivalent (7). Several derivatives containing both neutral and anionic axial ligands have been reported. Analytical data for these complexes, which most likely retain the sulfate-bridged, metal-metal bonded structure, were reported together with the original structure report (8). Finally, another platinum(III) sulfate complex, **2**, that contained dimethylsulfoxide coordinated to the axial positions and was more stable and soluble than its aqua counterpart, was structurally characterized in 1981 (12). The Pt-Pt distance of

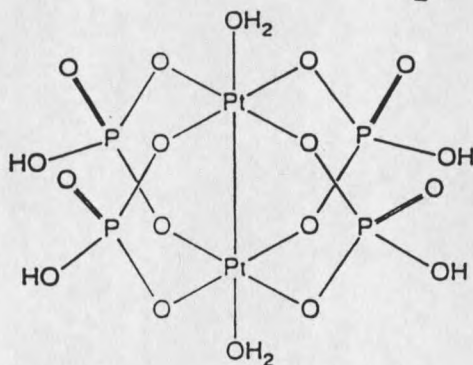
2.471(1) Å was not significantly different from that reported for  $K_2[Pt_2(SO_4)_4(H_2O)_2]$ .



### Phosphate-Bridged Complexes

Several dimeric platinum(III) phosphate complexes, **3**, that are structurally similar to their sulfate analogues were prepared and subsequently characterized in 1982 (11, 13-16). These complexes were structurally very similar to the sulfate complexes in that they have four bridging ligands, two axial ligands, and relatively short metal-metal single bonds ranging from 2.486(1) to 2.529(1) Å.

3



These complexes were more stable and soluble than their sulfate analogues. However they were similar in that it typically has been difficult to substitute the bridging phosphate groups for other ligands without breaking the metal-metal bond (16). One exception to this trend was the reaction of  $(\text{pyrH})[\text{Pt}_2(\text{HPO}_4)_4(\text{pyr})_2]$  with triphenylphosphine in water, which apparently led to a product in which one of the phosphate bridges has been replaced with two triphenylphosphine ligands (16). This complex, formulated as  $[\text{Pt}_2(\text{HPO}_4)_3(\text{PPh}_3)_2(\text{H}_2\text{O})_2]$ , has not been structurally characterized by X-ray crystallography. The only type of reaction of these complexes that has been clearly demonstrated was substitution of the axial ligands. A variety of derivatives have been prepared with pyridine or substituted pyridine molecules as axial ligands. Most other reactions attempted tended to break the metal-metal bond leading to decomposition of the complex. A similar situation occurred with the sulfate complexes.

$^{195}\text{Pt}$  Nuclear Magnet Resonance (NMR) data have been reported for many of the sulfate- and phosphate-bridged complexes discussed above (17, 18). For complexes with two different axial ligands, the Pt-Pt coupling constants were measured directly from the AB portions of the spectra. The  $^1\text{J}(\text{Pt-Pt})$  coupling constants were larger in magnitude for complexes with phosphate bridges than for those with sulfate bridges. However, the  $\nu(\text{Pt-Pt})$  from Raman spectra and the Pt-Pt bond lengths do not indicate stronger Pt-Pt bonds for the phosphate complexes (18). The authors conclude that the  $^1\text{J}(\text{Pt-Pt})$  in these

complexes must be extremely sensitive to variations in electronic structure which has little effect on the molecular structure.

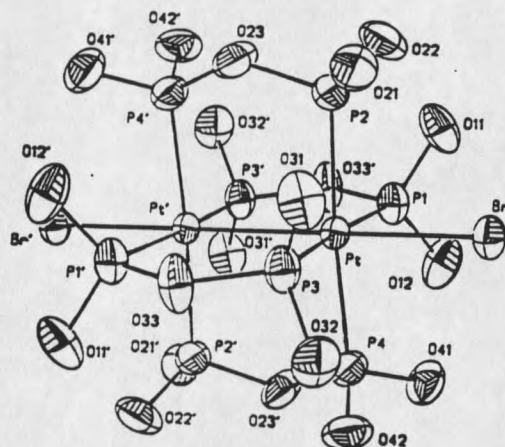
### Diphosphite Bridged Complexes

In 1977, the reaction of  $K_2[PtCl_4]$  with molten phosphorous acid was reported to yield a material that had an intense green luminescence upon irradiation with ultraviolet (UV) light (19). This complex was originally thought to be  $Pt(OP(OH)_2)_2(P(OH)_3)_2$ , first reported in 1961 (20). In the last twenty years, the luminescent species, which is now known as tetra- $\mu$ -pyrophosphitodiplatinum(II) ion,  $[Pt_2(pop)_4]^{4-}$ ,  $pop = P_2O_5H_2^{2-}$ , has been shown to exhibit many unusual properties. In 1982, Gray et al. (21) demonstrated that dimeric  $[Pt_2(pop)_4]^{4-}$  complexes would undergo oxidative addition reactions with halogens or methyl iodide, yielding dimeric platinum (III) complexes with the general formula  $[Pt_2(pop)_4X_2]^{4-}$ . In this report, the authors stated that oxidative addition to dimeric platinum (II) complexes with concomitant formation of a Pt-Pt single bond was an energetically favorable process. The formation of a Pt-Pt single bond apparently drove these reactions, where two  $\sigma$ -anti-bonding Pt-Pt electrons were transferred to  $X_2$  from the  $[Pt_2(pop)_4]^{4-}$ , which had a  $\sigma^2\sigma^{*2}$  configuration. This reaction resulted in a  $\sigma^2$  ground state for the  $Pt(III)_2$  complex. In accordance with this interpretation was the observed shortening of the Pt-Pt bonds in the  $[Pt_2(pop)_4X_4]^{4-}$  complexes relative to the sulfate- and phosphate-bridged

complexes. Moreover, the electronic absorption spectra of these complexes supported this interpretation. An intense two-band pattern, attributable to transitions from the  $d\sigma^2$  ground state, was observed in the spectrum of each complex. The higher energy, more intense component has been assigned to a  $d\sigma \rightarrow d\sigma^*$  transition (21).

Di-adducts,  $[\text{Pt}_2(\text{pop})_4\text{X}_2]^{4-}$ , with  $\text{Br}^-$  (22, 23),  $\text{I}^-$  (22),  $\text{NO}_2^-$  (24, 25),  $\text{SCN}^-$  (25, 26), and imidazolyl (25) have been synthesized, as well as the mixed adducts,  $[\text{Pt}_2(\text{pop})_4\text{XY}]^{4-}$ , where  $\text{X} = \text{Cl}^-, \text{Br}^-, \text{I}^-$ ; and,  $\text{Y} = \text{Cl}^-, \text{Br}^-, \text{I}^-, \text{CN}^-, \text{NO}_2^-$  (24, 26, 27). These species have been formed by using coordinating oxidizing agents, separate oxidizing and coordinating agents, electrochemical oxidation, or substitution reactions (24, 27). Of the 15 complexes,  $[\text{Pt}_2(\text{pop})_4\text{XY}]^{4-}$  ( $\text{X} = \text{Y} = \text{Cl}^-, \text{Br}^-, \text{I}^-, \text{NO}_2^-, \text{SCN}^-, \text{imidazolyl}$ ;  $\text{X} = \text{Cl}^-, \text{Y} = \text{Br}^-, \text{NO}_2^-$ ;  $\text{X} = \text{Br}^-, \text{Y} = \text{CN}^-, \text{NO}_2^-$ ;  $\text{X} = \text{I}^-, \text{Y} = \text{Cl}^-, \text{Br}^-, \text{CH}_3^-, \text{NO}_2^-, \text{CN}^-$ ), prepared, only nine have been structurally characterized ( $\text{X} = \text{Y} = \text{Cl}^-$  (28, 21),  $\text{Br}^-$  (22, 23),  $\text{I}^-$  (22),  $\text{NO}_2^-$  (24, 30),  $\text{SCN}^-$  (30), imidazolyl (30);  $\text{X} = \text{I}^-, \text{Y} = \text{CH}_3^-$  (25)). All of these complexes have similar structures, with four diphosphite ligands bridging the two metal centers and the axial positions occupied by either  $\text{Cl}^-/\text{Cl}^-$ ,  $\text{Br}^-/\text{Br}^-$ ,  $\text{I}^-/\text{I}^-$ ,  $\text{NO}_2^-/\text{NO}_2^-$ ,  $\text{SCN}^-/\text{SCN}^-$ , or  $\text{CH}_3^-/\text{I}^-$  (21-23, 25, 29, 30). The larger metal-metal distances as compared to the sulfate- and phosphate-bridged complexes have been attributed to the larger chelate distance of the diphosphite ligand, which is due to steric interactions between the phosphorus atoms. A representative structure, **4**, is shown below.

4

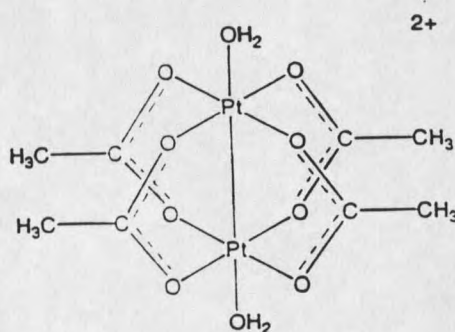


### Acetate and Acetylacetonate Bridged Complexes

The lantern-type dimeric Pt(III) complex, tetra- $\mu$ -acetatodiplatinum(III) dication, was not successfully synthesized until 1992 by Appleton et al. (31). There was an earlier report in 1980 of a synthesis by Rudyi et al. (32) in which hexahydroxoplatinum(IV) was reduced with formic acid in glacial acetic acid. The only characterization of the Rudyi et al. complex was through elemental analysis, and Appleton et al. commented on their inability to reproduce the Rudyi et al. synthesis. To date, this is the last platinum lantern complex to be synthesized for which other analogous metal ion complexes have been well characterized, e.g., rhodium(II) acetate (33).

The reported synthesis of the tetra- $\mu$ -acetatodiplatinum(III) dication is similar to the syntheses of the sulfate- and phosphate-bridged complexes. A solution of  $K_2[Pt(NO_2)_4]$  in a 2:1 mixture (v:v) of glacial acetic acid and 1 M perchloric acid was heated in air. The complex was obtained as a yellow solid,

and elemental analysis suggested the complex  $[\text{Pt}_2(\text{CH}_3\text{CO}_2)_4(\text{H}_2\text{O})_2](\text{ClO}_4)_2$ , **5**. The authors observed violent decompositions of the above complex. They also demonstrated that the reaction would proceed using with 1 M trifluoromethanesulfonic acid, yielding the analogous trifluoromethanesulfonate salt.

**5**

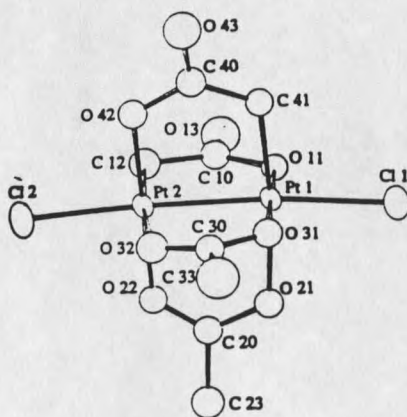
X-ray crystal structure determination showed that the complex was dimeric and exhibited many similarities to the neutral rhodium complex. The most obvious difference was that the Pt-OH<sub>2</sub> bond was much shorter (2.167(12) Å) (31) than the Rh-OH<sub>2</sub> bond (2.310 Å) (33). However, the bond distance was very similar to those in the sulfate (2.111(7) Å) (11) and phosphate (2.161(13) Å) (14) dimeric platinum(III) complexes. Another distinction was the Pt-Pt bond distance (2.3905(14) Å) in the diaquato complex, which was the shortest Pt-Pt single bond distance published to date. A more typical bond distance was the one found in the tetra- $\mu$ -sulfatodiaquadiplatinum(III) dianion (2.461(1) Å) (11). The bond



distance for the tetra- $\mu$ -acetato complex with chloride in the axial positions is more typical (2.451(1) Å).

In an attempt to synthesize the tetra- $\mu$ -acetato complex, Yamaguchi et al. synthesized the mixed bridged complex  $[\text{Pt}_2(\mu\text{-CH}_2\text{COO-C,O})_2(\mu\text{-CH}_3\text{COO-O,O}')_2\text{Cl}_2]^{2-}$  (34), **6**. Although platinum complexes can contain Pt-C bonds, such C,O-bridging modes were unprecedented. This complex has been well characterized.  $^{13}\text{C}$  NMR spectrum in  $\text{D}_2\text{O}$  revealed that the complex contained two types of acetate ligands. One peak of the NMR spectrum was at higher magnetic field with a large  $^1\text{J}[\text{Pt-C}]$  coupling constant (22.30 ppm;  $^1\text{J}[\text{Pt-C}] = 665$  Hz), while the other peak resembled a more typical acetate  $\text{CH}_3$  resonance (6.80 ppm;  $^2\text{J}[\text{Pt-C}] = 53$  Hz).

**6**

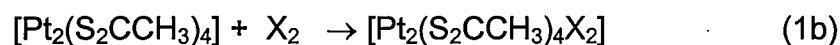
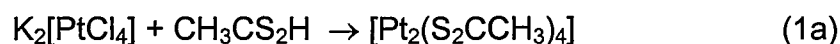


X-ray structure determination of **6** was fully consistent with the NMR data. The two  $\text{CH}_2\text{COO}^{2-}$  ligands are mutually *cis*, and each Pt atom was coordinated

by one carbon and three oxygen atoms, as well as one apical chloride ion. The Pt-Pt metal distance (2.451 Å) fit well with the other Pt(III) dimers.

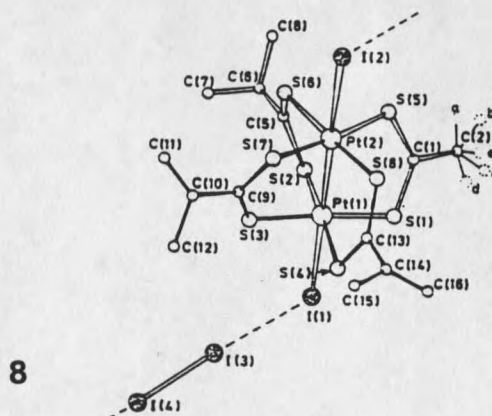
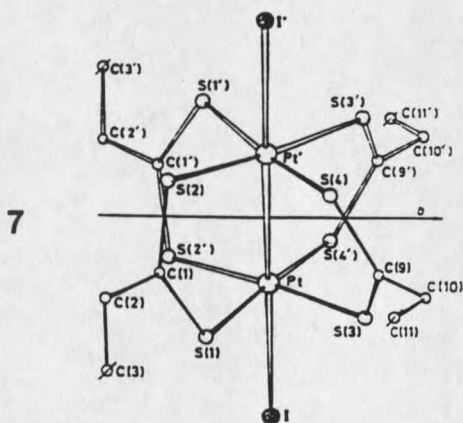
### Dithiocarboxylate Bridged Complexes

Another report of halogen oxidation of a binuclear platinum(II) complex occurred in 1983. Bellitto et al. (35) prepared a series of dimeric platinum(III) dithioacetate complexes of the general formula  $[\text{Pt}_2(\text{S}_2\text{CCH}_3)_4\text{X}_2]$  by halogen oxidation of the binuclear platinum(II) precursor,  $[\text{Pt}_2(\text{S}_2\text{CCH}_3)_4]$  (Equation 1).



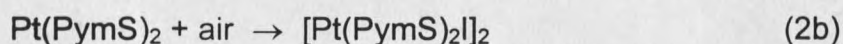
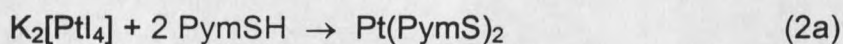
These complexes were not very soluble in common organic solvents, and single crystals could not be grown for X-ray crystallography. The authors based their formulations on elemental analysis and infrared (IR) spectra. The dimeric nature of these complexes was inferred from their vibrational spectra, parts of which were superimposable on both the  $[\text{Pt}_2(\text{S}_2\text{CCH}_3)_4]$  (36) and  $[\text{Pd}_2(\text{S}_2\text{CCH}_3)_4]$  (37) spectra for which a dimeric structure had been established. These complexes were, in principle, rather easy to prepare. However, the dimeric precursor was formed in rather low yields and must be prepared from  $\text{CH}_3\text{CS}_2\text{H}$ , which was very difficult to synthesize in pure form. For these reasons, the complexes were not studied further.

In another paper, Bellitto et al. (38) described the synthesis and properties of two other dimeric platinum(III) dithiocarboxylate complexes. Using a method analogous to the one used for the synthesis of the dithioacetate complex, the authors were able to prepare the dithiophenylacetate complex,  $[\text{Pt}_2(\text{S}_2\text{CCH}_2\text{Ph})_4\text{I}_2]$ , as well as the dithioisobutanoate complex,  $[\text{Pt}_2(\text{S}_2\text{CCHMe}_2)_4\text{I}_2]$ . These complexes were much more soluble in non-polar or weakly polar organic solvents than the analogous dithioacetate complex. The complexes, which have iodine atoms coordinated to the axial positions, crystallized in two different forms, one of which included molecular iodine in the unit cell. The molecular structures consisted of dimeric Pt-Pt units bridged by four dithiocarboxylate groups, with the axial positions in all cases being occupied by iodine atoms. The metal-metal distances were 2.598(2) Å and 2.578(1) Å for  $[\text{Pt}_2(\text{S}_2\text{CCH}_2\text{Ph})_4\text{I}_2]$ , **7**, and  $[\text{Pt}_2(\text{S}_2\text{CCHMe}_2)_4\text{I}_2]\cdot\text{I}_2$ , **8**, respectively. The air stability and high solubility of these complexes suggested that they might be useful for further studies.



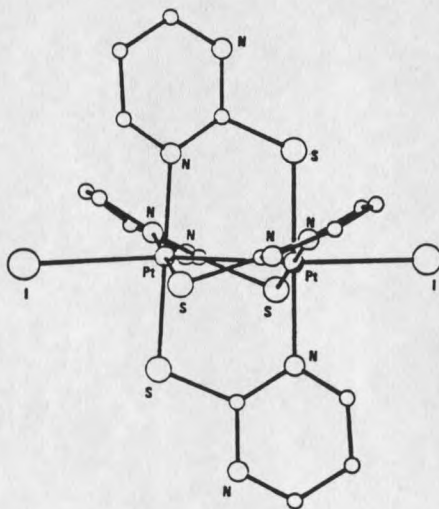
Pyrimidine-thionate and Pyridine-thiol Bridged Complexes

In 1984, Goodgame et al. reported the facile synthesis of a dimeric platinum(III) complex by direct reaction of pyrimidine-2-thione (PymSH) with  $K_2[PtI_4]$  (39) (Equation 2).



The initially formed  $Pt(\text{PymS})_2$  complex was air stable only as a dry solid; however, in the presence of air the initially yellow precipitate rapidly re-dissolved to form a crimson solution. X-ray structure determination of the dimeric platinum(III) complex (**9**) showed that the complex forms a *cis*-planar array of two sulfur and two nitrogen atoms around platinum with an iodine atom apical.

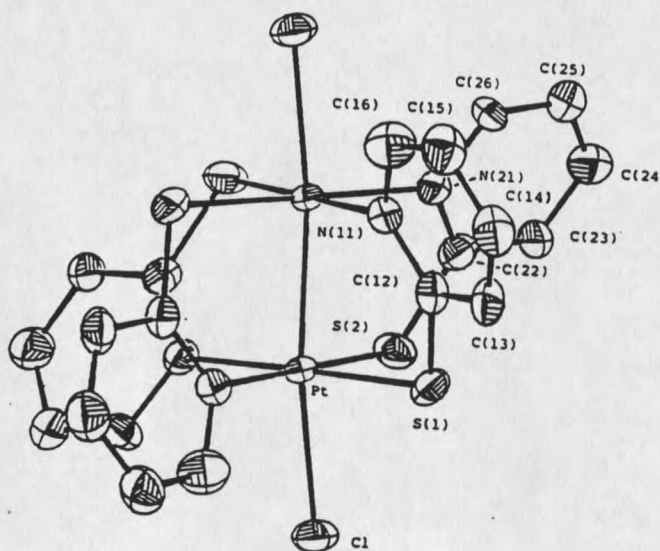
**9**



The  $\text{PtN}_2\text{S}_2$  planes were not fully eclipsed; there exists ca.  $26^\circ$  twist about the Pt-Pt axis. Five of the atoms coordinated to each platinum are in a closely octahedral arrangement, but the iodine atoms were displaced ca.  $7^\circ$  from the Pt-Pt axis. This displacement was due primarily to steric interactions with the pyrimidine rings. The Pt-Pt distance ( $2.544 \text{ \AA}$ ) fell between those of quadruply-bridged Pt(III) dimers with O-donors ( $2.466 - 2.494 \text{ \AA}$ ) (12, 16) and that for quadruply-bridged Pt(III) dimers with P-donors ( $2.695 \text{ \AA}$ ) (21).

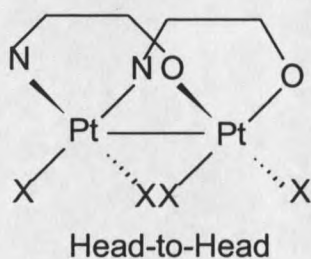
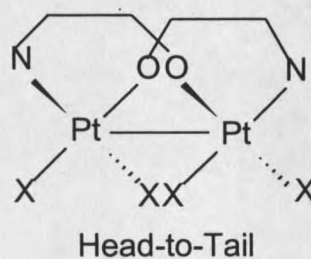
Umakoshi et al. synthesized  $[\text{Pt}_2(\text{Pyt})_4\text{Cl}_2]$  (where Pyt = pyridine-2-thiol), **10**, in 1987 (40), a complex analogous to the Goodgame complex. The  $\text{PtN}_2\text{S}_2$  coordination square had a *cis* configuration, and the coordination squares were twisted toward each other about the Pt-Pt axis (torsion angle =  $23.3^\circ$ ). The Pt-Pt bond distance ( $2.532(1) \text{ \AA}$ ) was very similar to that of **9**.

10



### Doubly-Bridged Dimeric Pt(III) Complexes

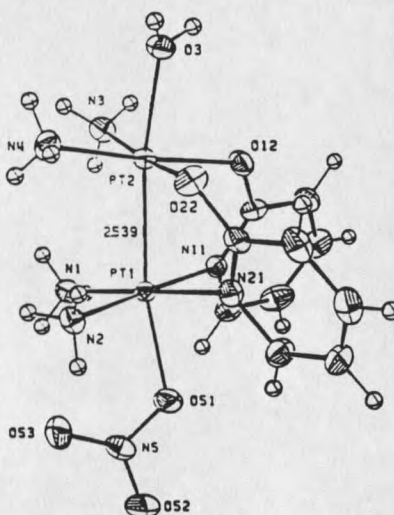
Unlike lantern-type dimeric Pt(III) complexes, doubly-bridged dimeric Pt(III) complexes contain only two bridging ligands, typically in a *cis* conformation, and two monodentate ligands *trans* to the bridging ligands. Furthermore, fewer complexes of this type are observed than the large variety of transition metal ions found in lantern-type complexes, e.g., Cu, Cr, Mo, W, Tc, Re, Ru, Os, Rh, Ir, Ni, Pd, and Pt. Complexes of this type have more variety in the manner in which they form. Bridging ligands in these cases tend to have two different coordinating atoms, e.g., N, O; P, O; S, O, etc. This allows the ligands to bridge in two non-identical ways: head-to-head (HH) or head-to-tail (HT). For example, if a bridging ligand has N and O as coordinating atoms, the following two complexes, **11a** and **11b**, may form:

**11a****11b**

where X = halogen, alkyl, amine, or nitrogen-containing ligand and N<sup>^</sup>O is a bridging ligand.

$\alpha$ -Pyridone and Pyrimidine Bridged Complexes

Several different dimeric platinum(III) complexes with  $\alpha$ -pyridone or pyrimidine bases have been prepared by chemical or electrochemical oxidation of either tetranuclear, mixed-valent platinum blues or the related binuclear platinum(II) species (41-45). The structures of these complexes have two  $\alpha$ -pyridone or pyrimidine ligands in a *cis* orientation and two *cis* amino groups coordinated to each metal center. These ligands, which are asymmetric, can bridge the Pt-Pt bond in either a head-to-head (HH) or in a head-to-tail (HT) fashion. The axial positions can be occupied by a variety of ligands such as  $\text{H}_2\text{O}$ ,  $\text{NO}_3^-$ ,  $\text{NO}_2^-$ ,  $\text{Cl}^-$ , or  $\text{Br}^-$ . An example, **12**, with  $\alpha$ -pyridone ligands is shown below:

**12**

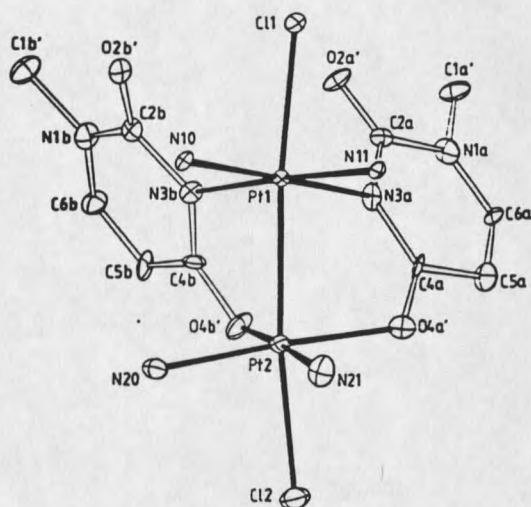
The metal-metal distances for the various adducts ranged from 2.539(1) Å to 2.582(6) Å (41-45). The Pt-Pt distances were typically longer than those of the tetra-bridged complexes because of the presence of only two bridging ligands. Furthermore, there was a substantial twist around the metal-metal bond due to

steric interactions between the *cis* amino groups on the respective metal centers. Although several different dimeric platinum(III) complexes have been prepared, the synthetic methods used to prepare the precursors have proven to be rather unpredictable. Platinum blues cannot typically be formed in high yields and tend to be rather unstable in solution (41-45).

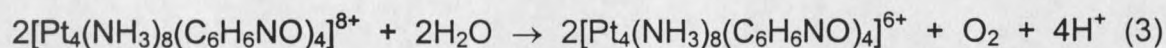
The formation of metal-metal bonds in the head-to-head and head-to-tail  $\alpha$ -pyridonate bridged dimeric platinum(III) complexes has been studied electrochemically using cyclic voltammetry, differential pulse voltammetry, and controlled-potential coulometry (44). These studies revealed that the Pt-Pt bond was formed in either a concerted two-electron charge transfer process (HT complexes) or through two one-electron steps (HH complexes) (44). Both oxidations are coupled to chemical reactions, which complicated the analysis. This was not unexpected, as the dimeric platinum(III) products have two coordinated axial ligands that were not present in the starting dimeric platinum(II) complexes.

There have been several recent reactivity studies with dimeric platinum(III) products derived from platinum blues. In one study (46), it was shown that two of the  $\text{NH}_3$  ligands of the 1-methyluracil dimeric platinum(III) complex, *cis*- $[\text{Pt}_2(\text{NH}_3)_4(\text{meu})_2\text{Cl}_2]\text{Cl}_2 \cdot 3.5\text{H}_2\text{O}$ , **13**, could be replaced readily by chloro ligands.





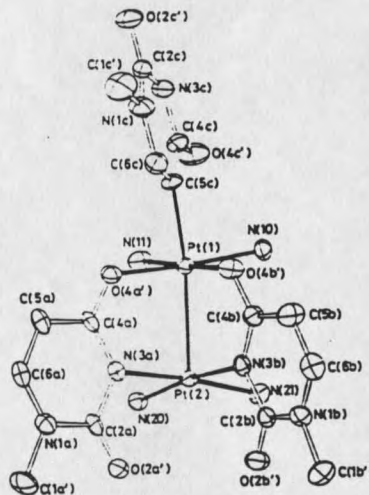
In another study (47), a tetranuclear platinum(III) complex with  $\alpha$ -pyrrolidone bridging ligands, was isolated and was shown to oxidize water to molecular oxygen (Equation 3).



A unique dimeric platinum(III) complex containing one penta-coordinated and one hexa-coordinated platinum atom was recently synthesized (48). This complex consisted of two *cis*-( $\text{NH}_3$ )<sub>2</sub>Pt<sup>3+</sup> moieties bridged by two 1-methyluracilato ligands in a HH fashion and a third 1-methyluracilato ligand coordinated to one of the platinum atoms through its C(5) position, 14. The authors noted that this complex represented the first example of a Pt-nucleobase complex that contained a Pt-C bond. In addition, this complex was the first

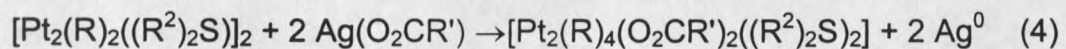
structurally characterized dimeric platinum(III) complex with unequal coordination of the platinum atoms.

14



### Carboxylate Bridged Complexes

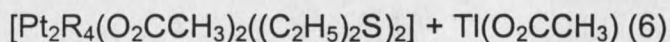
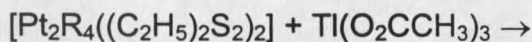
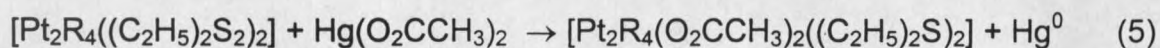
The use of silver salts to oxidize a binuclear Pt(II) complex was first reported in 1978 (49, 50). A series of complexes with two bridging carboxylate groups and two alkyl or aryl groups coordinated in a *cis* configuration about the two platinum atoms was reported (Equation 4):



where R = Me, Ph, p-toyl; R' = Me, CF<sub>3</sub>; R<sup>2</sup> = Et, Pr. The starting materials were proposed to be dimeric complexes with the two *cis*-Pt(R)<sub>2</sub> units bridged by the (R<sup>2</sup>)<sub>2</sub>S ligands (51, 52). These compounds were used successfully with a variety

of silver carboxylates and typically produced dimeric platinum(III) complexes with many of the properties desired for further studies. Oxidation of the binuclear platinum(II) starting materials was not limited to the use of silver salts.

Mercury(II) and thallium(III) carboxylate salts have also been used to prepare carboxylate bridged platinum(III) complexes (Equations 5 and 6) (49, 50):

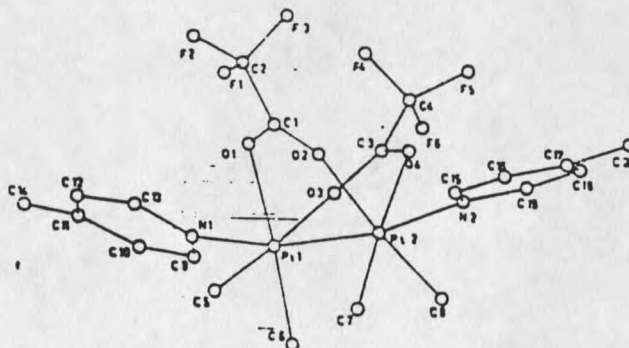


where R = CH<sub>3</sub>, Ph, or p-tolyl. Indeed, the platinum(II) complexes with aryl groups reacted much faster with thallium(III) acetate than with silver acetate.

One complex, which was prepared with the use of silver trifluoroacetate,

$[\text{Pt}_2(\text{CH}_3)_4(\text{O}_2\text{CCF}_3)_2(p\text{-NC}_6\text{H}_7)_2]$ , was characterized by x-ray crystallography (53),

15.



15

This complex was structurally very similar to the  $\alpha$ -pyridonate complexes discussed above and has a Pt-Pt bond length of 2.557(1) Å. The dimeric unit was bridged by two carboxylate groups, and each platinum was coordinated by two methyl groups in a *cis* arrangement. In a manner similar to that in the  $\alpha$ -pyridonate complexes, there was a torsional twist about the metal-metal bond due to steric repulsion between the methyl groups. The axial sites can be occupied by a variety of suitable donor ligands such as pyridine, 4-picoline, and trialkyl or aryl phosphines, arsines, and stilbenes (49).

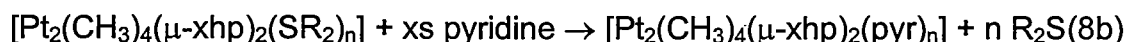
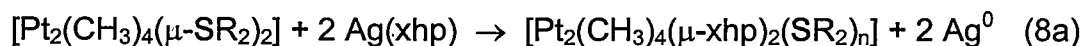
Asymmetric carboxylate-bridged complexes with one axial ligand can be prepared if only one equivalent of the donor ligand per molecule was added (Equation 7):



where  $\text{L} = \text{P}(\text{Et})_3$  or  $\text{P}(\text{OMe})_3$  and  $\text{R} = \text{CH}_3$ , Ph, or *p*-tolyl. The asymmetric nature of these complexes was determined from  $^{31}\text{P}$  NMR, which showed one main signal together with two sets of  $^{195}\text{Pt}$  satellites due to direct and long range coupling. Currently, none of these asymmetric carboxylate-bridged complexes have been characterized by X-ray crystallography.

### Hydroxypyridinate-Bridged Complexes

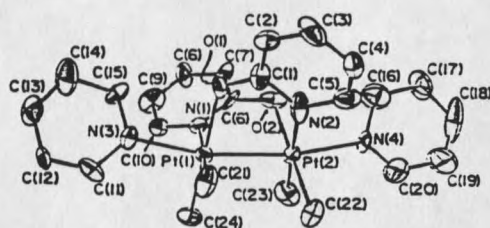
Using a variation of the Vrieze method, Cotton et al. were able to prepare a series of dimeric Pt(III) complexes that contained two *cis*-hydroxypyridine bridges and methyl groups *trans* to the bridging ligands (54-56). The complexes are readily prepared by the following reaction (Equation 8).



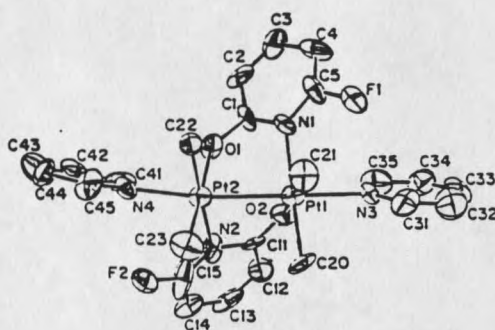
where R = C<sub>2</sub>H<sub>5</sub>; x = H, F, Cl, Br, or CH<sub>3</sub>, and n = 1 or 2. The axial position occupation varied with x. The larger the substitution on the hydroxypyridine the more steric interference that hindered one of the axial sites. When x = CH<sub>3</sub>, the resultant complex had one platinum atom that is 5-coordinate and one which is 6-coordinate.

X-ray structure determination on all four derivatives exhibited interesting characteristics about the complexes. When x = H or F, a head-to-tail (HT) arrangement was found, **16** and **17**. In this case, both axial positions were accessible for coordination. The axial positions were occupied by pyridine, and the Pt-Pt distances are 2.550(1) Å and 2.551(2) Å, respectively.

16

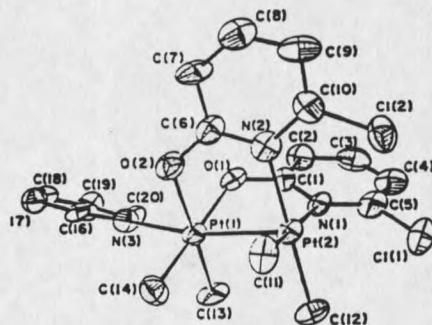


17

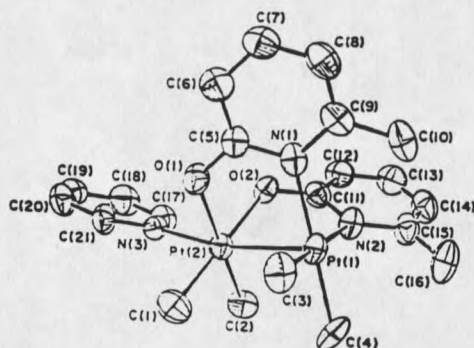


When  $x = \text{Cl}$  or  $\text{CH}_3$ , a head-to-head arrangement occurred. In this case, only one axial site was occupied due to steric hindrance, **18** and **19**. A single pyridine molecule occupied the axial position, and the Pt-Pt bond lengths were slightly shorter (2.543(2) Å and 2.545(1) Å, respectively) compared to **16** and **17**. The Pt-N (pyridine) bond distances (2.060(11) Å and 2.030(8) Å, respectively) were much shorter than those in which both axial sites were occupied (2.183(24) Å and 2.20(1) Å, respectively).

18

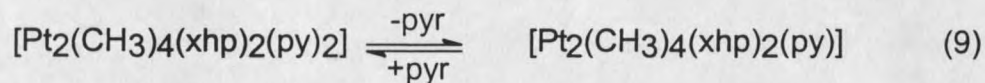


19



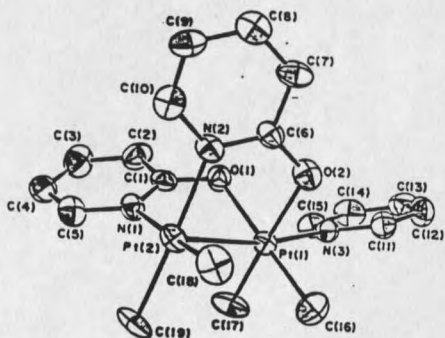
Cotton et al. published two more reports in which they synthesized the HH complexes with  $x = \text{H}$ , F and Br, **20-22**, (55) and the HH complexes with  $x = \text{H}$ , F,  $\text{CH}_3$  with a single diethyl sulfide molecule in the axial position, **23-25**, (56). In their previous publication (54), Cotton et al. commented that when  $x = \text{H}$  or F the complex adopted a HT arrangement while when  $x = \text{Cl}$  or  $\text{CH}_3$  the arrangement

was HH. At the time these observations seemed reasonable due to steric arguments; however, the authors found that the following process could occur (Equation 9) (55).

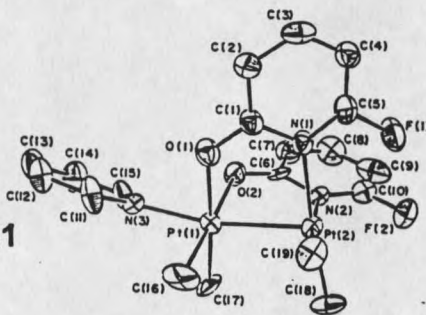


Removal of a pyridine was accomplished by passing the complex through a silica gel chromatography column and evaporating the eluent to dryness. To add pyridine to the HH complex, the complex was dissolved, and an excess of pyridine was added. The analogous diethyl sulfide capped complexes were formed as shown in Equation 8a.

20

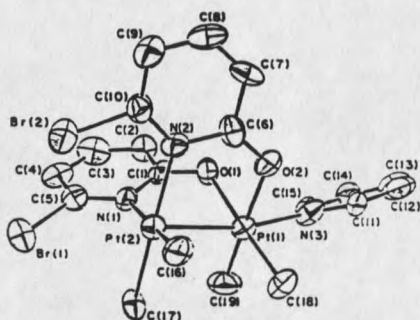


21

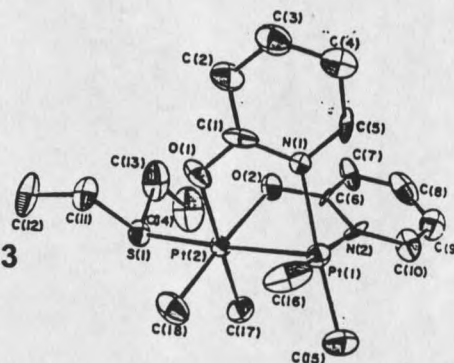




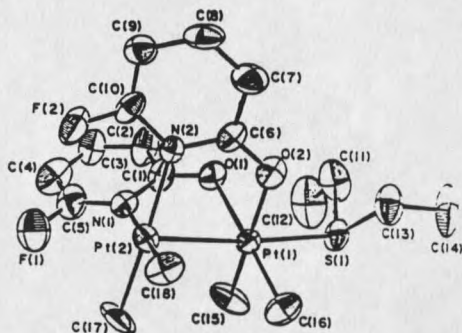
22



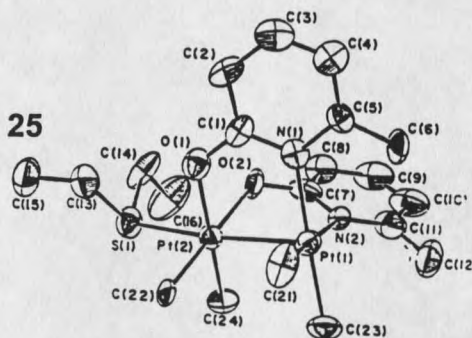
23



24



25



In a unique equilibrium study, Abbott et al. studied the equilibrium and the mechanism of the hydroxypyridine derivatives' rearrangement (57). The HT complex was in fast exchange with pyridine while the HH complex was in slow exchange. The equilibrium constant was determined by integrating the pyridine  $\alpha$ -proton resonance, which provides the ratio of HH complex to the total HT complex plus free pyridine, and the well-separated region of the 5-H resonances

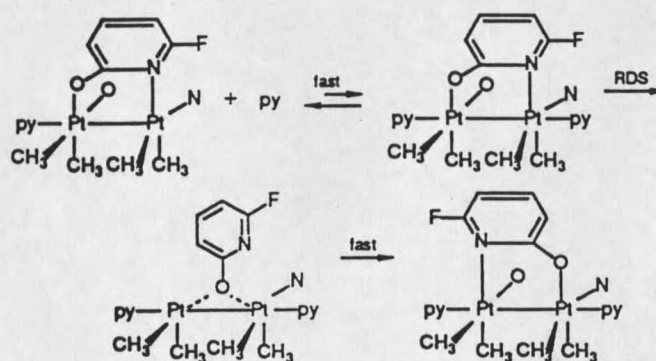
of the xhp, which provided the ratio of HH to HT complex. Abbott et al. was then able to calculate all of the relevant concentrations from these measurements. To study the mechanism of rearrangement, the complex concentrations were varied from 0 to 10 mM, and the pyridine concentrations were varied from 0 to 0.5 M.

The authors were able to calculate the rearrangement equilibria for  $x = H$  and  $F$  ( $120 \text{ L mol}^{-1}$  and  $25 \text{ L mol}^{-1}$ , respectively) from the following (Equation 10).



No rearrangement attributable to the steric bulk of the  $x$ -substituent was observed for  $x = \text{Cl}$  or  $\text{CH}_3$ . Using the fluorinated-derivative, fhp, the authors studied the mechanism of HH to HT rearrangement. By varying the pyridine concentrations, the reaction was determined to be first order in pyridine and in complex. Addition of free mhp to the reaction mixture did not show any formation of a mixed mhp, fhp complex even after 20 half-lives. The authors suggested the following mechanism (Scheme 1).

Scheme 1



### Other Dimeric Pt(III) Complexes

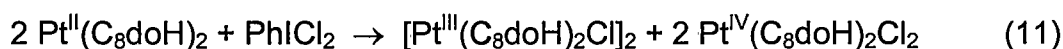
A series of papers were published by Muraveiskaya et al. describing peroxy- and hydroxy-bridged dimeric platinum(III) complexes derived from the same reaction mixture as the sulfate complexes (58-61). This work has been disputed on several grounds and has not been substantiated by X-ray crystal analysis. Much of the work was not reproducible and most of the complexes have unlikely formulations that are based solely on IR and XPS and potentiometric titrations. At present, there was not enough solid evidence to conclude that these complexes actually contain platinum in the +3 oxidation state. A similar series of papers by Rudyi et al. described the preparation of  $\text{Pt}_2(\text{O}_2\text{CCH}_3)_6$  by the reduction of  $\text{K}_2\text{Pt}(\text{OH})_6$  in  $\text{CH}_3\text{COOH}$  by  $\text{HCOOH}$  (62, 63). This work has been found not to be reproducible as reported. Products were obtained that did not have reproducible microanalyses corresponding to those of the original report, suggesting that the products were either polymeric or impure.

Finally, a series of papers describing the preparation of platinum acetamide complexes (64-66) were published. These complexes have at various times been identified as containing platinum in the +2, +3, and +4 oxidation states. Recent XPS studies suggest that the platinum atoms in these complexes were equivalent and in the +3 oxidation state. The most likely, and currently accepted, formulation of these complexes is  $[\text{Pt}_2(\text{CH}_3\text{CONH})_4\text{X}_2]$  where  $\text{X} = \text{Cl}, \text{Br}, \text{I}, \text{NO}_3, \text{or } \text{NO}_2$ . Unfortunately, using current methods of synthesis, it has been proven impossible to grow single crystals for X-ray diffraction studies.

### Unbridged Dimeric Pt(III) Complexes

These complexes are unique in that they do not contain bridging ligands that support the two metal centers. Before the discovery of unbridged Pt(III) dimers, scientists believed that the formation of a Pt(III) dimer was an exceptionally rare occurrence. Although the number of complexes that form in this manner is relatively low, the future of Pt(III) chemistry has changed dramatically with their discovery.

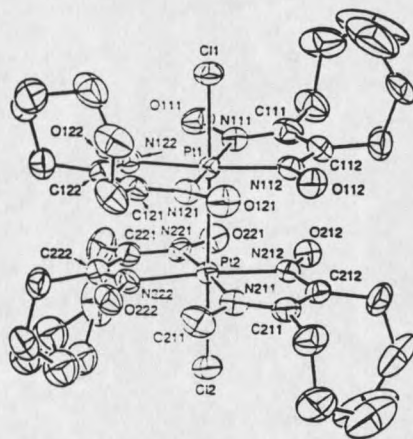
Baxter et al. synthesized the first such complex in 1992 (67). In what has been deemed an unusual and unexpected result, carbocyclic  $\alpha$ -dioximato ( $C_8doH$ ) was reacted with  $K_2[PtCl_4]$  to produce the planar Pt(II) complex,  $Pt(C_8doH)_2$ . Using  $PhICl_2$  as an oxidant, the complex undergoes oxidative-addition of chloride. The oxidant produced not only the Pt(III) complex but also an equi-molar amount of a Pt(IV) complex as follows (Equation 11).



The two products were isolated chromatographically from a basic alumina column. X-ray crystal structure determination, **26**, showed that the two  $Pt(C_8doH)_2$  units were mutually rotated by  $63.5(3)^\circ$ . The  $PtN_4$  moiety was approximately planar, while the extended carbocyclic segments were not restricted to planarity and fold outward, offering no hinderance to dimerization.

Each axial position was occupied by chloride. The Pt-Pt bond length (2.694(1) Å) was the longest platinum bond distance published at that time.

26

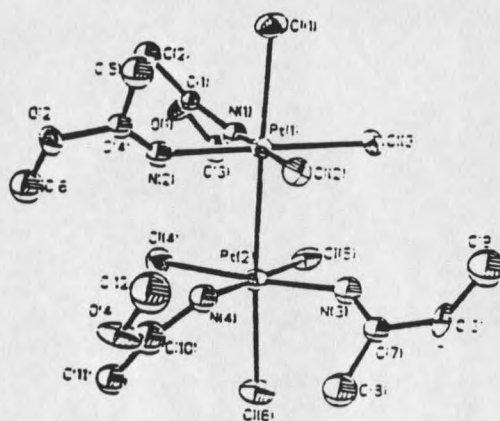


In 1996, Prenzler et al. described the second unbridged dimeric Pt(III) complex (68). The complex was composed of two substituted acetylacetonate ligands  $(R(CO)CH(CO)R')$  where  $R/R' = Me/Me, Me/CF_3$  or  $Ph/Ph$  and a chloride ion coordinated to each platinum atom. The complex was not structured by X-ray crystallography, however, the complex was characterized by other methods: a) electrospray mass spectroscopy; b) Raman spectroscopy; and, c)  $^{195}Pt$  and  $^1H$  NMR spectroscopy. The molecular ion  $[Pt_2(acac)_4Cl_2] \cdot M^+$  (where  $M = H^+$  or  $Na^+$ ) was observed as well as abundant fragment ions  $[Pt_2(acac)_4Cl]^+$  and  $[MeCNPt_2(acac)_4]^+$ . The prominent Raman-active band at  $144\text{ cm}^{-1}$  was a very characteristic Pt-Pt symmetric stretching vibration. Additionally, the NMR data were consistent with the previous data, and the mononuclear Pt(II) or Pt(IV)

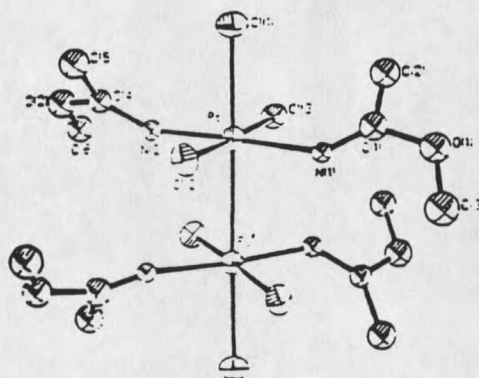
complex provide significantly different data. To date, no X-ray structure determination of this complex has been published.

In 1997, Bandoli et al. published two more structures that did not contain bridging ligands, *cis*- and *trans*-bis[bis(imino-methoxyethane)trichloroplatinum(III)], **27** and **28**, (69). These complexes were neutral dimers composed of two planar PtCl<sub>2</sub>L<sub>2</sub> units, perpendicularly connected by a Pt-Pt bond and capped axially by chloride ligands. The iminoether ligands have the expected E configuration with extensive electron charge delocalization over the N--C--O moiety, and all non-hydrogen atoms were near planar. The Pt-Pt bond lengths (2.765(2) Å and 2.758(3) Å for *cis* and *trans*, respectively) were greater than values reported earlier for the dioximato complex synthesized by Baxter et al.. This difference was significant; the Pt-Pt lengthening was unlikely to have an electronic origin and was most likely caused by steric repulsion between the imino ligands.

27

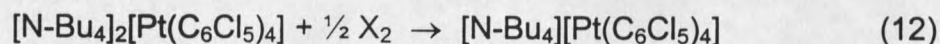


28



### Mononuclear Pt(III) Complexes

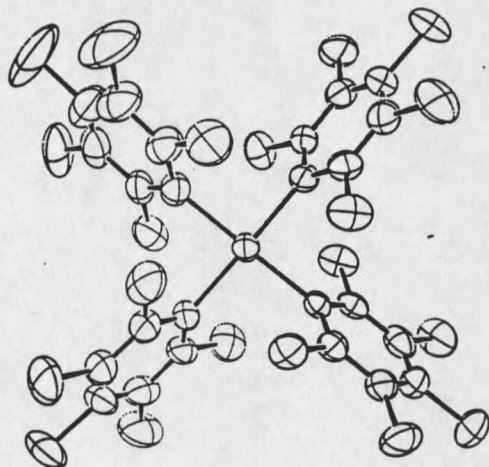
To date, there has been one published example of a fully characterized mononuclear platinum(III) complex. This was reported in 1984 by Uson et al. and was prepared as follows:



where  $\text{X} = \text{Cl}^-$ ,  $\text{Br}^-$ , or  $\text{I}^-$  (70). The resulting complex was deep blue, paramagnetic, and air and moisture stable. X-ray crystal structure determination, **29**, showed it to be square planar with almost identical geometry to the platinum(II) precursor. The stability of this unusual complex has been attributed to the presence of the unique  $\text{C}_6\text{Cl}_5$  ligand. Although there have been other

reports of syntheses of mononuclear platinum(III) compounds, this was the only such complex that has been fully characterized to date.

29





## EXPERIMENTAL METHODS

Preparation of ComplexesStarting Materials

Potassium tetrachloroplatinate(II) ( $K_2[PtCl_4]$ ), silver(I) salts,  $AgX$ , ( $X = BF_4$ ,  $CF_3SO_3$ ) and cadmium nitrate ( $Cd(NO_3)_2$ ) were obtained from Johnson Matthey and used as supplied. Silver(I) hexafluorophosphate ( $AgPF_6$ ) was purchased from Acros and used as supplied. All remaining chemicals were purchased from Aldrich Chemicals and used as supplied. Various solvents were used and stored over 4 Å molecular sieves to remove ambient water contamination. The following solvents were obtained from Fischer Scientific: toluene ( $C_7H_8$ ) ACS-grade; chloroform ( $CHCl_3$ ) HPLC-grade; acetonitrile ( $CH_3CN$ ) HPLC-grade; methanol ( $CH_4O$ ) HPLC-grade; acetone ( $C_3H_6O$ ) HPLC-grade; and, dichloromethane ( $CH_2Cl_2$ ) HPLC-grade. Fischer Scientific also supplied the following potassium salts:  $KCl$ ;  $KBr$ ;  $KCN$ ; and  $KI$  that were all ACS-grade. Cambridge Isotope Laboratories, Inc supplied all the deuterated solvents (water- $d_2$ ; chloroform- $d_1$ ; dichloromethane- $d_2$ ; acetone- $d_6$ ; acetonitrile- $d_3$ ; and, benzene- $d_6$ ) that were used for the NMR studies and stored over 4 Å molecular sieves (organic solvents only).

Tetramethylbis( $\mu$ -diethyl sulfide)diplatinum(II) (30) and Tetramethylbis( $\mu$ -dipropyl sulfide)diplatinum(II) (31).

The complexes were prepared by the literature method (71).

Tetramethylbis( $\mu$ -dimethyl sulfide)diplatinum(II) (32).

The complex was prepared by the literature method (72).

Bipyridyldimethylplatinum(II) (33) and Dimethylphenanthrolineplatinum(II) (34).

The complexes were prepared by the literature method of Puddephatt et al. (73).

Biquinolinedimethylplatinum(II) (35).

The complex was prepared as a variation of Puddephatt et al. (73). The ligand, biquinoline, was substituted for the diimines, 2,2'-bipyridyl and 1,10-phenanthroline. The yield was comparable to complexes **33** and **34** at 89%.

Bis(bipyridyl)tetramethylbis(pyridyl)diplatinum(III) dication (36) and

Tetramethylbis(phenanthroline)bis(pyridyl)diplatinum(III) dication (37).

Both complexes were prepared in the same manner as illustrated by the following example. Dissolve **33** (20.2 mg, 53.0  $\mu$ mole) into acetonitrile (10 mL). Pyridine (42  $\mu$ L, 0.53 mmole) was added to the solution and the mixture was stirred magnetically. A solution of silver(I) triflate (13.6 mg, 53.0  $\mu$ mole) in acetonitrile (3 mL) was then added to the platinum solution. The solution color changed from orange-red to yellow upon addition of the silver(I) solution. The mixture was then stirred for approximately 2 hours. The colloidal silver was removed by passing the reaction mixture through a plug of Celite and the resulting yellow solution was transferred into a round bottom flask, cooled to 0 °C in an ice bath and the solvent was removed under high vacuum. The solid was redissolved into dichloromethane and once again the solvent was removed under high vacuum. The resultant yellow powder was reprecipitated by dissolving the solid into a minimal amount of dichloromethane and adding to a large excess of ether. Yield: **36**: 98%, 31.7 mg, 26.0  $\mu$ mole; **37**: 97%. Anal. Calcd for  $C_{36}H_{38}F_6N_6O_6Pt_2S_2$ : C, 35.47; H, 3.14; F, 9.35; N, 6.89; S, 5.26. Found: C, 35.20; H, 3.52; F, 9.48; N, 7.28; S, 5.96. Anal. Calcd for  $C_{40}H_{38}F_6N_6O_6Pt_2S_2$ : C, 37.92; H, 3.02; N, 6.63. Found: C, 37.62; H, 3.03; N, 6.64.

Substitution of axial ligands on 36 and 37.

Two different methods were used to study the substitution of axial ligands on **36** and **37**. One method required the preparation of solutions of the **36** or **37** as described above. After the removal of the colloidal silver from the reaction mixture, various equivalents of triphenylphosphine ( $\text{PPh}_3$ ),  $\text{SCN}^-$ , and  $\text{Cl}^-$  were added as either pure acetonitrile solutions as with the first two ligands or acetonitrile solutions with a minimal amount of water added to dissolve the salts. The second method used solid **36** and **37** dissolved into acetonitrile and the addition of the same ligands.

Mixture of 36, 37, and Bipyridyltetramethylphenanthrolinebis(pyridyl)-diplatinum(III) dication (38).

A solution of **33** (10.8 mg, 28.3  $\mu\text{mole}$ ) and **34** (11.5 mg, 28.4  $\mu\text{mole}$ ) in acetonitrile (15 mL) was magnetically stirred. A 50 fold excess of pyridine (225  $\mu\text{L}$ , 2.84 mmole) and silver triflate (14.6 mg, 56.8  $\mu\text{mole}$ ) was added and the reaction was left to stir for one hour. The reaction solution was passed through a plug of Celite and the solution was then used as is. Proton NMR shows complete conversion to the mixed dimers in a statistical yield of 1:2:1 **36:38:37**.

Tetramethylbis(phenanthroline)bis(thiocyanato)diplatinum(III) (39).

**34** (20.6 mg, 50.8  $\mu\text{mole}$ ) was dissolved into acetonitrile (20 mL) and was magnetically stirred. A solution of NaSCN (53.7 mg, 0.662 mmole) in acetonitrile (5 mL) was added to the stirred solution. Silver triflate (13.1 mg, 51.0  $\mu\text{mole}$ ) in acetonitrile (2 mL) was added and the mixture is left to stir at room temperature for 72 hours. The reaction mixture was then filtered through Celite, cooled in an ice bath and the solvent is removed under high vacuum. The solid is washed with dichloromethane and removed under high vacuum. The complex, **39**, was reprecipitated in the same manner as **36** and **37**. (Yield 23.2 mg, 25.0  $\mu\text{mole}$ , 98%)

Thermodynamic Study

A thermodynamic study of the interconversion between the dimeric forms of **30**, **31** and **32** and their respective monomers was performed. Standard solutions of each of the dimers and the respective free dialkylsulfide ( $\text{SR}_2$ ) were prepared in dichloromethane- $\text{d}_2$ . Constant concentrations of the dimer and varying equivalents of  $\text{SR}_2$  were then added to a 1 mL volumetric flask and further diluted. Constant volumes were added to 5 mm NMR tubes. A total of eight samples were prepared for each dimer at each temperature. Equilibrium

was achieved in a matter of minutes for R = Me but required 3 hr for R = Pr at the lowest temperature studied as demonstrated by proton NMR. Concentrations of all species in each equilibrium reaction were readily obtained by integrating the well-separated methyl or methylene on sulfur and methyl on platinum resonances in each system. Equilibrium constants were measured over the temperature range 283 to 308 K for each system and  $\Delta H$  and  $\Delta S$  were calculated from van't Hoff plots (R values of 0.999).

### Kinetic Analysis

A kinetic study for the formation of the two dimeric platinum(III) complexes, **36** and **37**, was performed by monitoring the reaction by  $^1\text{H}$  NMR. Standard solutions of **33** and **34** (26 mM), silver(I) triflate (52 mM) and **36** (84 mM) were prepared. Constant volumes of platinum and silver were used throughout the study. The first variable studied was pyridine. The reactions were set-up in a pseudo-first order fashion and the pyridine concentration was varied from a 3- to 100-fold excess. The next variable studied was silver(I). The concentrations of silver(I) were varied from 0.10 to 1.5 equivalents per platinum. The third variable to be determined was the effect of the dimeric platinum(III) product, **36**. Varying equivalents of **36** were added to a constant 50-fold excess pyridine mixture. The final variable was the effect of silver(0). This was

accomplished by two methods: 1) using a previously silvered NMR tube or 2) addition of a 5 cm piece of 30 gauge silver wire to the NMR tube. The pyridine concentration was held constant at a 50-fold excess. Integrals of the methyl on platinum (**33** or **34**) were monitored by  $^1\text{H}$  NMR and standardized to an internal standard of TMS. First order plots of the integral versus time were made for each reaction. Five reactions were performed for each reaction condition and the temperature was held constant at 298 K.

#### Methyl Migration Study

Standard solutions of **33** were prepared in acetonitrile- $\text{d}_3$ . Solutions containing Hg(II) acetate, Cd(II) triflate, Zn(II) sulfate and Zr(IV) oxide dichloride were also prepared in acetonitrile- $\text{d}_3$ . Samples from the stock solution of **33** (0.5 mL) was transferred into a 1.0 mL volumetric flask. Various equivalents of the metals (Hg(II), Cd(II), Zn(II), and Zr(IV)) were added and finally diluted to volume. Constant volumes from the resulting solution were added 5 mm NMR tubes.

#### Instrumental Methods

##### Nuclear Magnetic Resonance

$^1\text{H}$  NMR spectra were acquired on Bruker AC300, AM500 FT spectrometers or on Avance DRX-250, DPX-300 or DRX-500 FT spectrometers

operating at 5.85 T, 7.02T or 11.7 T. All chemical shifts were referenced to either the residual protio-solvent peak or to an internal standard of TMS. Standard parameters were used unless otherwise noted.

### Ultraviolet-Visible Spectroscopy

UV-Vis spectra were recorded on a Hewlett Packard 8453 spectrophotometer. Beer's Law studies were performed on **33** and **36** by varying the concentrations from 500  $\mu\text{M}$  to 3.13  $\mu\text{M}$ . A Job's study was performed using 250  $\mu\text{M}$  **33** and **36**.

### Electron Paramagnetic Resonance

EPR Spectra were obtained on a Bruker ESR 220D-SCR spectrometer at liquid  $\text{N}_2$  temperatures. Standard procedures were used to determine adequate power levels to be used to collect data. Four scans were run at a time constant of 200 sec. All spectra were obtained under the same gain and modulation settings. Double integrals were calibrated with a 1 M Cu(II) triethonamine standard in acetonitrile.



## RESULTS AND DISCUSSION

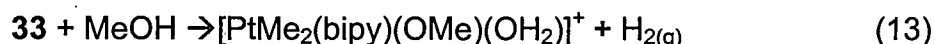
The following sections present all of the results of this research. The goal of the project was to investigate the reactivity of dimethyl platinum(II) complexes and their ability to form one-dimensional polymers. Although the initial complexes that were studied did not prove to be well chosen, the complexes with the diimine ligands, 2,2'-bipyridyl (bipy) and 1,10-phenanthroline (phen), have shown many interesting reactions. Discussion of pertinent literature was also included where such discussion served to further clarify the interpretation of these results.

Starting Materials: PtMe<sub>2</sub>(bipy) and PtMe<sub>2</sub>(phen)

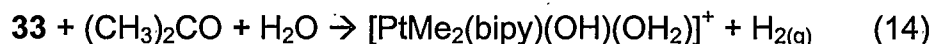
The red complexes, PtMe<sub>2</sub>(bipy) (**33**) and PtMe<sub>2</sub>(phen) (**34**), were prepared by Puddephatt et al. (73). These sixteen electron complexes are very electron rich and have been shown to be among the most reactive complexes of the noble metals (74). They undergo oxidation, oxidative-addition and oxidative-addition/reductive-elimination reactions. The reactivities of **33** and **34** played very important roles in the chemistry that has been developed through this research.

Reactivity of the PtMe<sub>2</sub>(diimine) complexes

The two complexes, diimine = bipy (**33**) or phen (**34**), have been shown to be very reactive towards oxidative-addition chemistry (73, 74). The complexes react at room temperature with alcohols, ROH where R = Me, Et, 2-Pr, to produce the respective axial alkoxy/aqua platinum(IV) complex (73). For example:

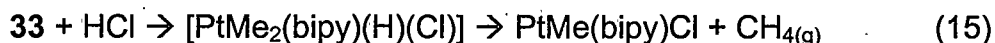


The alkoxy-ligand (e.g. MeO) formed a robust bond. There was no evidence of exchange when dissolved into CD<sub>3</sub>OD or in D<sub>2</sub>O, since the methoxy signal with <sup>195</sup>Pt coupling was still observed in the <sup>1</sup>H NMR spectrum. Furthermore, a D<sub>2</sub>O solution can be made 0.1 M in HClO<sub>4</sub>, and the MeOPt group was still unchanged. When **33** or **34** was dissolved in acetone and treated with water, a Pt(IV) complex that has axial sites containing OH/OH<sub>2</sub> was formed.



An oxidative-addition reductive-elimination of methane reaction occurred when PtMe<sub>2</sub>(diimine) was reacted with acid. The mechanism of this reaction was described by Puddephatt et al. (74). When **33** or **34** was reacted with HX, where X may be Cl<sup>-</sup> or NO<sub>3</sub><sup>-</sup>, a Pt(IV) complex was formed with X<sup>-</sup> and H<sup>+</sup> in the axial

sites. This complex then quickly underwent a reductive-elimination of methane and the Pt(II) complex, PtMeX(diimine), was obtained.



### Crystal Structures of the PtMe<sub>2</sub>(diimine) complexes and derivatives

In the article describing the preparation of the two PtMe<sub>2</sub>(diimine) complexes, Puddephatt stated that red crystals formed in solution, but no X-ray crystal structure analysis was performed (73). During my preparation of the complexes, crystals were obtained and analyzed. Figures 1 and 2 show the ORTEP diagram of PtMe<sub>2</sub>(bipy), **33** and PtMe<sub>2</sub>(phen), **34**, respectively. Crystallographic data for the two complexes, **33** and **34**, is presented below.

A year after my structure determination of **33**, an article was published that contained the X-ray structure determination of **33** (75). The published bond lengths and bond angles were the same as those found in my structure determination. The bond lengths and angles of **33** and **34** are similar. However, in comparison to the bridged dinuclear Pt(II) complex, Pt<sub>2</sub>(μ-N-acetyl-L-cysteine-S)<sub>2</sub>(bipy)<sub>2</sub>, the Pt-N bond lengths are noticeably longer in **33** and **34**. The bond length for the thiolate bridged complex is 2.01(2) Å (76) compared to those presented here, 2.1 (1) Å in **33** and 2.098(7) Å in **34**. The Pt-N bond length

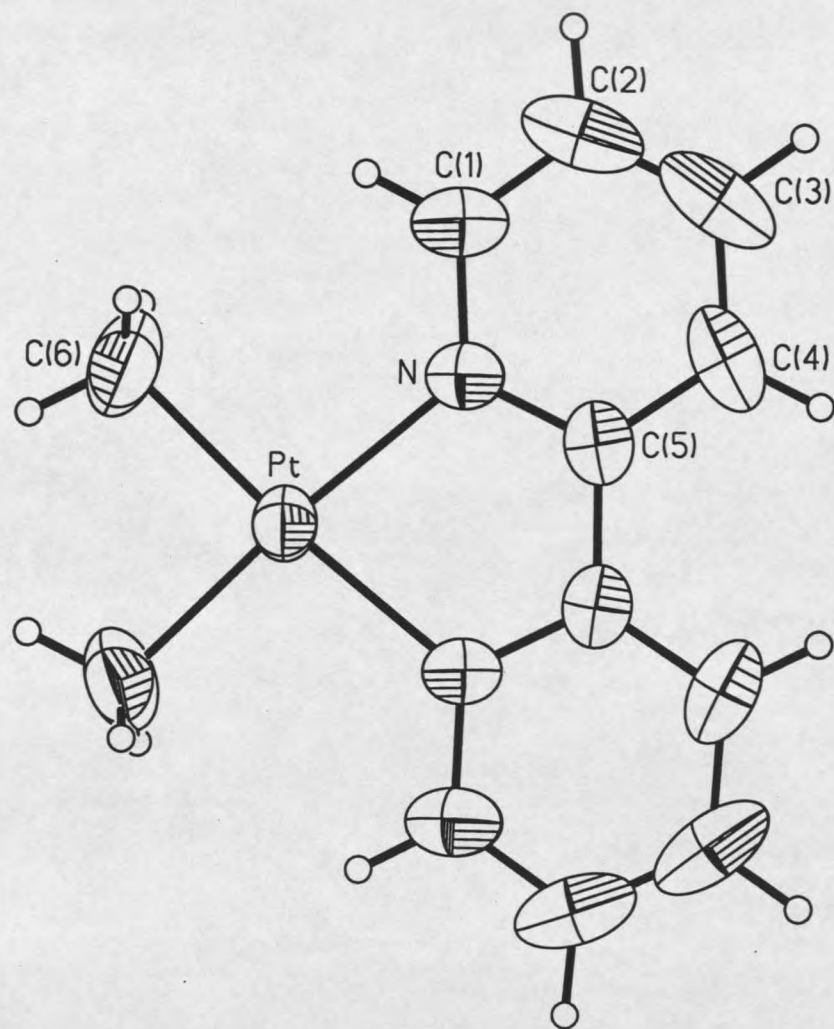


**Figure 1.** Thermal ellipsoid plot of **33** showing 50% probability ellipsoids and numbering scheme for the structure.

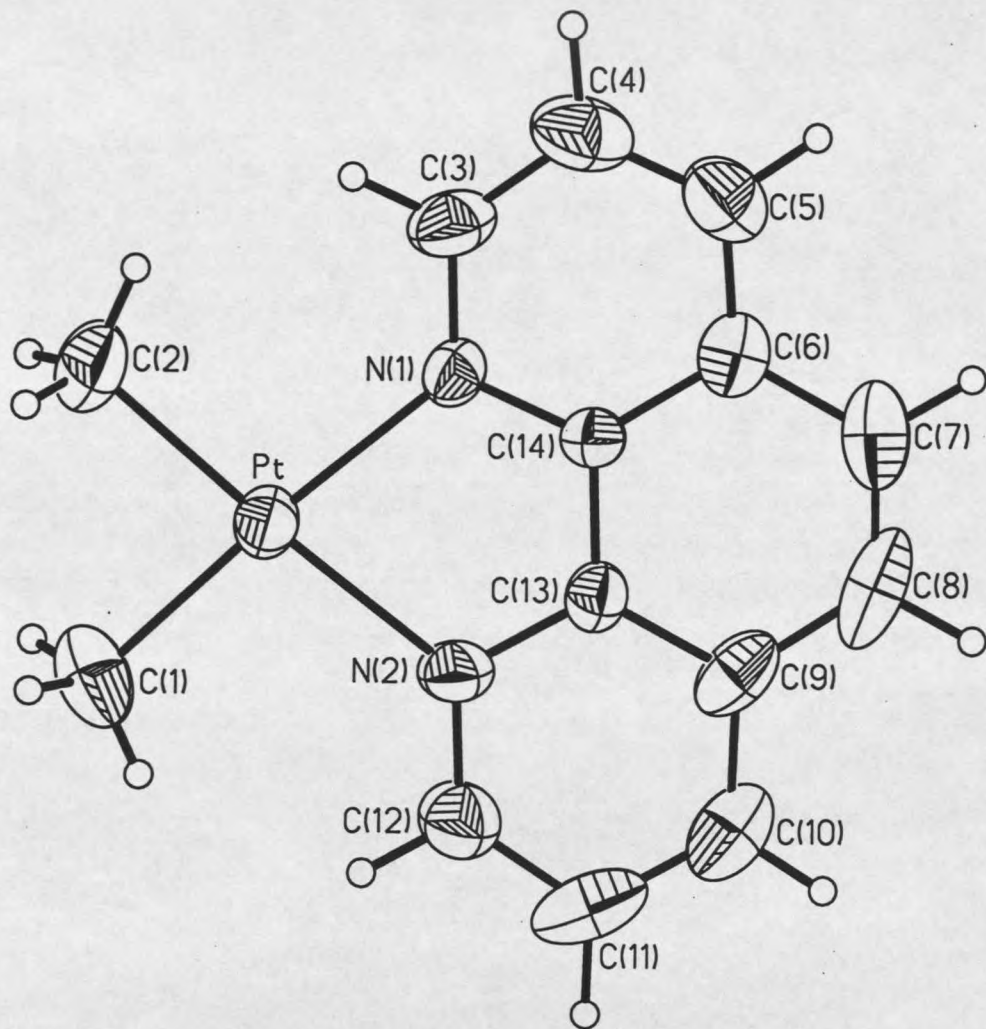


**Figure 2.** Thermal ellipsoid plot of **34** showing 50% probability ellipsoids and numbering scheme for the structure.

**Table 1.** Crystallographic data for PtMe<sub>2</sub>(bipy) (**33**) and PtMe<sub>2</sub>(phen) (**34**).

Parameter	<b>33</b>	<b>34</b>
Formula	C <sub>12</sub> H <sub>14</sub> N <sub>2</sub> Pt	C <sub>14</sub> H <sub>14</sub> N <sub>2</sub> Pt
Formula weight	381.3	405.4
Space Group	C2/c	P2 <sub>1</sub> /c
Unit cell: a (Å)	17.596(2)	9.244(1)
b (Å)	9.530(2)	12.591(2)
c (Å)	7.174(2)	7.744(1)
β (°)	110.85(2)	107.37(1)
volume (Å <sup>3</sup> )	1124.2(4)	1201.8(4)
Z	4	4
ρ (g cm <sup>-3</sup> ) calculated	2.253	2.240
absorption coef, Mo K <sub>α</sub> (cm <sup>-1</sup> )	124.5	116.5
F(000)	712	760

**Table 2.** Data collection and structure refinement data for **33** and **34**.

Parameter	<b>33</b>	<b>34</b>
2 $\theta$ range ( $^{\circ}$ )	4-75	4-75
Unique reflections	2970	2326
Observed reflections	1205	1658
Number of parameters	69	154
Trans. Factor range	0.225-0.651	0.050-0.123
Final R <sup>a</sup> , observed data	0.060	0.040
Final wR <sup>b</sup> , observed data	0.047	0.040
Final wR <sup>b</sup> , all data	0.060	0.046
Goodness of fit	1.26	1.29
<sup>a</sup> $R = \sum    F_o  -  F_c    / \sum  F_o $ . <sup>b</sup> $wR = [\sum (w(F_o^2 - F_c^2)^2) / \sum wF_o^4]^{1/2}$ where $w = [\sigma^2(F) + 0.0007F^2]^{-1}$		

**Table 3.** Atomic Coordinates and equivalent isotropic displacement coefficients for **33**.

Atoms	x/a	y/b	z/c	U(eq)
Pt	0.50000	0.27957(6)	0.25000	0.0425(2)
N	0.4224(5)	0.4499(9)	0.227(1)	0.045(3)
C(1)	0.3426(6)	0.444(1)	0.205(1)	0.063(5)
C(2)	0.2970(8)	0.5665(2)	0.196(2)	0.085(7)
C(3)	0.3311(9)	0.690(2)	0.209(2)	0.084(7)
C(4)	0.4130(8)	0.700(1)	0.228(2)	0.065(5)
C(5)	0.4575(6)	0.578(1)	0.240(1)	0.043(4)
C(6)	0.4169(8)	0.125(1)	0.225(2)	0.079(7)

**Table 4.** Bond lengths (Å) for **33**.

Bond	Length(Å)	Bond	Length(Å)
Pt-C(6)	2.04(1)	Pt-N	2.09(8)
N-C(1)	1.36(1)	N-C(5)	1.36(1)
C(1)-C(2)	1.36(2)	C(2)-C(3)	1.36(3)
C(3)-C(4)	1.40(2)	C(4)-C(5)	1.39(2)
C(5)-C(5A)	1.45(2)		



**Table 5.** Bond angles (°) for **33**.

Atoms	Angles(°)	Atoms	Angles(°)
C(6)-Pt-N	97.3(4)	C(6)-Pt-C(6A)	87.4(8)
N-Pt-C(6A)	175.3(4)	C(6)-Pt-N(A)	175.3(4)
N-Pt-N(A)	78.1(4)	C(6A)-Pt-N(A)	97.3(4)
Pt-N-C(1)	126.6(7)	Pt-N-C(5)	115.1(6)
C(1)-N-C(5)	118.3(9)	N-C(1)-C(2)	123(1)
C(1)-C(2)-C(3)	120(1)	C(2)-C(3)-C(4)	119(2)
C(3)-C(4)-C(5)	119(1)	N-C(5)-C(4)	121(1)
N-C(5)-C(5A)	115.8(6)	C(4)-C(5)-C(5A)	123.(7)

**Table 6.** Anisotropic displacement coefficients ( $\text{\AA}^2$ ) for **33**.

Atom	$U_{xx}$	$U_{yy}$	$U_{zz}$	$U_{xy}$	$U_{xz}$	$U_{yz}$
Pt	0.0491(3)	0.0355(3)	0.0352(3)	0.0000	0.0197(2)	0.0000
N	0.038(4)	0.053(5)	0.043(5)	0.001(4)	0.015(4)	0.002(4)
C(1)	0.040(6)	0.081(9)	0.069(8)	-0.002(6)	0.020(6)	-0.002(7)
C(2)	0.051(8)	0.13(1)	0.077(9)	0.028(9)	0.026(7)	0.001(9)
C(3)	0.070(9)	0.12(1)	0.061(8)	0.051(9)	0.016(7)	-0.003(8)
C(4)	0.089(9)	0.052(8)	0.051(7)	0.027(6)	0.020(6)	0.002(5)
C(5)	0.055(6)	0.042(6)	0.027(5)	0.003(5)	0.011(4)	0.0003(39)
C(6)	0.10(1)	0.047(8)	0.010(1)	-0.020(7)	0.050(8)	-0.002(7)

The anisotropic displacement exponent takes the form:  $-2\pi^2(h^2a^{2*}U_{xx} + \dots + 2hka*b*U_{xy})$

**Table 7.** Atomic Coordinates and equivalent isotropic displacement coefficients for 34.

Atoms	x/a	y/b	z/c	U(eq)
Pt	0.28645(4)	0.15375(2)	0.10107(6)	0.0383(1)
C(1)	0.494(1)	0.1323(7)	0.276(2)	0.062(5)
C(2)	0.261(1)	0.0379(6)	0.081(2)	0.065(5)
N(1)	0.076(9)	0.1833(4)	-0.081(1)	0.034(3)
N(2)	0.295(1)	0.2730(5)	0.113(1)	0.048(3)
C(3)	-0.035(1)	0.1374(6)	-0.174(2)	0.052(5)
C(4)	-0.168(1)	0.1624(8)	-0.294(2)	0.062(5)
C(5)	-0.188(1)	0.2395(7)	-0.323(2)	0.057(5)
C(6)	-0.079(1)	0.2896(6)	-0.227(1)	0.042(4)
C(7)	-0.091(2)	0.3705(7)	-0.244(2)	0.062(5)
C(8)	-0.021(2)	0.4155(7)	-0.142(2)	0.069(6)
C(9)	0.154(2)	0.3857(6)	-0.021(2)	0.051(5)
C(10)	0.272(2)	0.4303(7)	0.088(2)	0.061(6)
C(11)	0.394(2)	0.3963(7)	0.208(2)	0.068(6)
C(12)	0.399(1)	0.3189(7)	0.212(2)	0.055(5)
C(13)	0.170(1)	0.3071(6)	-0.003(1)	0.034(4)
C(14)	0.054(1)	0.2583(5)	-0.106(1)	0.034(3)

**Table 8.** Bond lengths (Å) for **34**.

Bond	Length(Å)	Bond	Length(Å)
Pt-C(1)	2.02(1)	Pt-C(2)	2.05(1)
Pt-N(1)	2.098(7)	Pt-N(2)	2.101(8)
N(1)-C(3)	1.34(1)	N(1)-C(14)	1.34(1)
N(2)-C(12)	1.32(1)	N(2)-C(13)	1.38(1)
C(3)-C(4)	1.37(1)	C(4)-C(5)	1.38(2)
C(5)-C(6)	1.38(2)	C(6)-C(7)	1.43(2)
C(6)-C(14)	1.42(1)	C(7)-C(8)	1.35(2)
C(8)-C(9)	1.41(2)	C(9)-C(10)	1.40(2)
C(9)-C(13)	1.39(2)	C(10)-C(11)	1.37(2)
C(11)-C(12)	1.36(2)	C(13)-C(14)	1.41(1)

**Table 9.** Bond angles (°) for **34**.

Atoms	Angles(°)	Atoms	Angles(°)
C(1)-Pt-C(2)	86.0(4)	C(1)-Pt-N(1)	173.3(4)
C(2)-Pt-N(1)	97.7(4)	C(1)-Pt-N(2)	98.1(4)
C(2)-Pt-N(2)	175.8(4)	N(1)-Pt-N(2)	78.3(3)
Pt-N(1)-C(3)	128.4(7)	Pt-N(1)-C(14)	114.1(6)
C(3)-N(1)-C(14)	117.5(8)	Pt-N(2)-C(12)	130.6(7)
Pt-N(2)-C(13)	113.1(6)	C(12)-N(2)-C(13)	116.3(9)
N(1)-C(3)-C(4)	124(1)	C(3)-C(4)-C(5)	118(1)
C(4)-C(5)-C(6)	119(1)	C(5)-C(6)-C(7)	124(1)
C(5)-C(6)-C(14)	118(1)	C(7)-C(6)-C(14)	118(1)
C(6)-C(7)-C(8)	120(1)	C(7)-C(8)-C(9)	122(1)
C(8)-C(9)-C(10)	121(1)	C(8)-C(9)-C(13)	118(1)
C(10)-C(9)-C(13)	117(1)	C(9)-C(10)-C(11)	120(1)
C(10)-C(11)-C(12)	118(1)	N(2)-C(12)-C(11)	126(1)
N(2)-C(13)-C(9)	123(1)	N(2)-C(13)-C(14)	117(1)
C(9)-C(13)-C(14)	120(1)	N(1)-C(14)-C(6)	123(1)
N(1)-C(14)-C(13)	118(1)	C(6)-C(14)-C(13)	120(1)

**Table 10.** Anisotropic displacement coefficients for **34**.

Atom	$U_{xx}$	$U_{yy}$	$U_{zz}$	$U_{xy}$	$U_{xz}$	$U_{yz}$
Pt	0.0362(2)	0.0324(2)	0.0459(3)	0.0016(2)	0.0115(2)	0.0024(3)
C(1)	0.043(7)	0.074(9)	0.067(9)	0.010(6)	0.013(6)	0.023(7)
C(2)	0.069(9)	0.034(6)	0.09(1)	0.002(6)	0.011(8)	0.008(7)
N(1)	0.034(5)	0.029(4)	0.041(5)	0.002(3)	0.013(4)	-0.002(4)
N(2)	0.053(6)	0.037(5)	0.043(5)	-0.013(5)	-0.002(4)	0.001(5)
C(3)	0.049(7)	0.044(7)	0.061(8)	-0.015(5)	0.012(6)	-0.013(6)
C(4)	0.037(6)	0.08(1)	0.062(8)	-0.008(7)	0.009(6)	-0.019(8)
C(5)	0.047(7)	0.072(9)	0.049(7)	0.009(6)	0.008(6)	-0.001(7)
C(6)	0.043(6)	0.042(6)	0.049(7)	0.004(5)	0.024(5)	0.005(5)
C(7)	0.059(8)	0.057(8)	0.08(1)	0.024(6)	0.028(7)	0.020(7)
C(8)	0.1(1)	0.033(7)	0.1(1)	0.019(7)	0.06(1)	0.014(7)
C(9)	0.074(9)	0.031(6)	0.058(8)	-0.008(6)	0.037(7)	-0.001(6)
C(10)	0.07(1)	0.039(6)	0.09(1)	-0.003(7)	0.040(8)	-0.002(7)
C(11)	0.08(1)	0.056(8)	0.07(1)	-0.033(8)	0.040(9)	-0.028(8)
C(12)	0.051(8)	0.053(7)	0.054(8)	-0.008(6)	0.005(7)	0.005(6)
C(13)	0.040(6)	0.031(6)	0.034(6)	0.003(4)	0.012(5)	0.002(5)
C(14)	0.031(5)	0.032(5)	0.036(6)	-0.001(4)	0.006(4)	-0.004(5)

The anisotropic displacement exponent takes the form:  $-2\pi^2(h^2a^2U_{xx} + \dots + 2hka^*b^*U_{xy})$

(2.07(2) Å) of the Pt(CN)<sub>2</sub>(phen) complex was similar to **34** (77) while the Pt-N bond length in Pt(NCO)<sub>2</sub>(bipy) (78) and Pt(NCS)<sub>2</sub>(bipy) (77) (2.00(5) Å and 1.91(2) Å, respectively) were similar to the thiolate bridged complex. The differences in these bond lengths are attributed to the *trans*-influence of the methyl groups of **33** and **34** and the cyanide group of Pt(CN)<sub>2</sub>(phen).

The two complexes, Pt(bipy)Br<sub>2</sub>, **40**, and Pt(bipy)I<sub>2</sub>, **41**, were also obtained as single crystals and X-ray structure determinations were performed. These two complexes were formed while trying to crystallize the dication [Pt(bipy)<sub>2</sub>]<sup>2+</sup> using various counter-anions. Crystals were obtained from solutions that contained an excess of KBr and KI. The molecular structures of **40** and **41** are comparable to the structures reported for the monomeric units of [Cu(bipy)X<sub>2</sub>]<sub>4</sub> (X = Cl, Br) (80) and [Pt(bipy)Cl<sub>2</sub>]<sub>4</sub> (81) and analogous to the molecular structure of Pt(1'-methyl-2,4'-bipyridin-3'-ylium)Cl<sub>2</sub> (82) and the monomeric unit of [Cu(phen)Br<sub>2</sub>]<sub>4</sub> (83). Among these complexes, there are no significant differences between comparable bond lengths and angles. However, the crystal structures for **40**, **41** and the methylbipyridinium complex differ from the crystal structures of the others with regard to the nature of the interactions between monomeric units.

Complexes **40**, **41** and the methylbipyridinium complex exhibit only van der Waals interactions between neighboring molecules. The others show weak bonding between atoms of neighboring monomeric units to form polymeric chains in the crystal structures. In the copper complexes, the monomeric units are linked by weak Cu-Cl (3.025(1) Å and 3.106(1) Å) or Cu-Br (3.175(1) Å and

3.286(2) Å) bonds, giving the copper atoms a distorted octahedral coordination. The halogen bridged Cu-Cu distances are 3.802(1) Å and 3.876(1) Å for the chloro complex and 3.964(1) Å and 3.974(1) Å for the bromo complex.

Although Pt(II) does not form complexes with six donor ligands, weak Pt-Pt interactions between square-planar Pt(II) complexes occur with planar ligands. The red form of Pt(bipy)Cl<sub>2</sub> is an example. Weak Pt-Pt interactions link monomeric units in chains with a Pt-Pt separation of 3.45 Å. It is unlikely that an isostructural bromo or iodo complex could be prepared. The bromo complex would have a Pt-Pt distance of ca. 3.75 Å and any Pt-Pt interaction would be too weak to compensate for the approximately three percent larger unit cell volume compared to the structure of **40**. This is just exaggerated for the iodo complex **41**. A yellow form of Pt(bipy)Cl<sub>2</sub> has also been reported (84) with the nearest Pt-Pt distance (from powder diffraction data) of approximately 4.5 Å in the solid. Its structure is probably analogous to **40** and **41** with regard to intermolecular interactions.

ORTEP diagrams for the two neutral complexes, Pt(bipy)Br<sub>2</sub>, **40** and Pt(bipy)I<sub>2</sub>, **41**, are shown in Figures 3 and 4 respectively. The following tables contain the crystallographic data for both complexes.



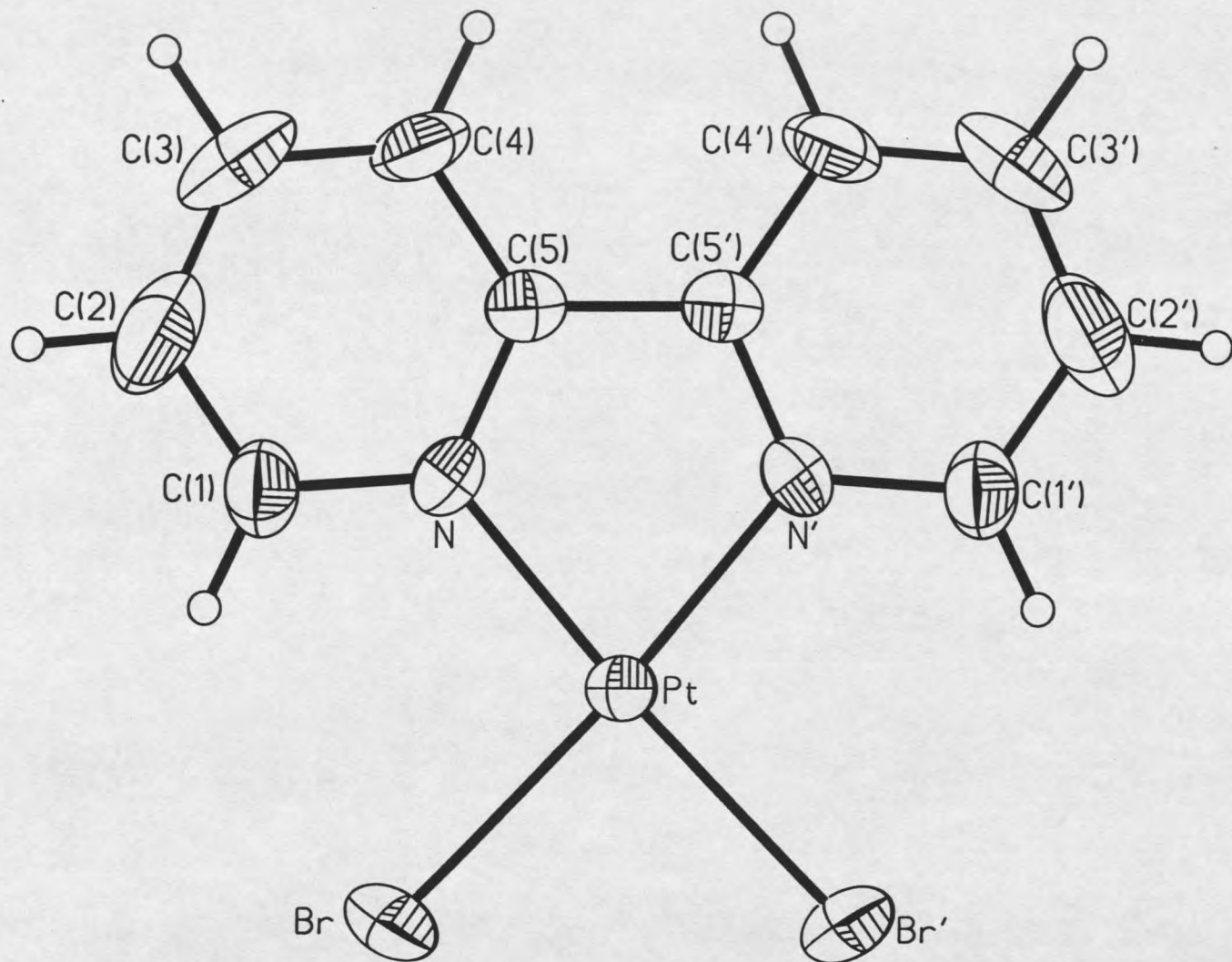


**Figure 3.** Thermal ellipsoid plot of **40** showing 50% probability ellipsoids and numbering scheme for the structure.

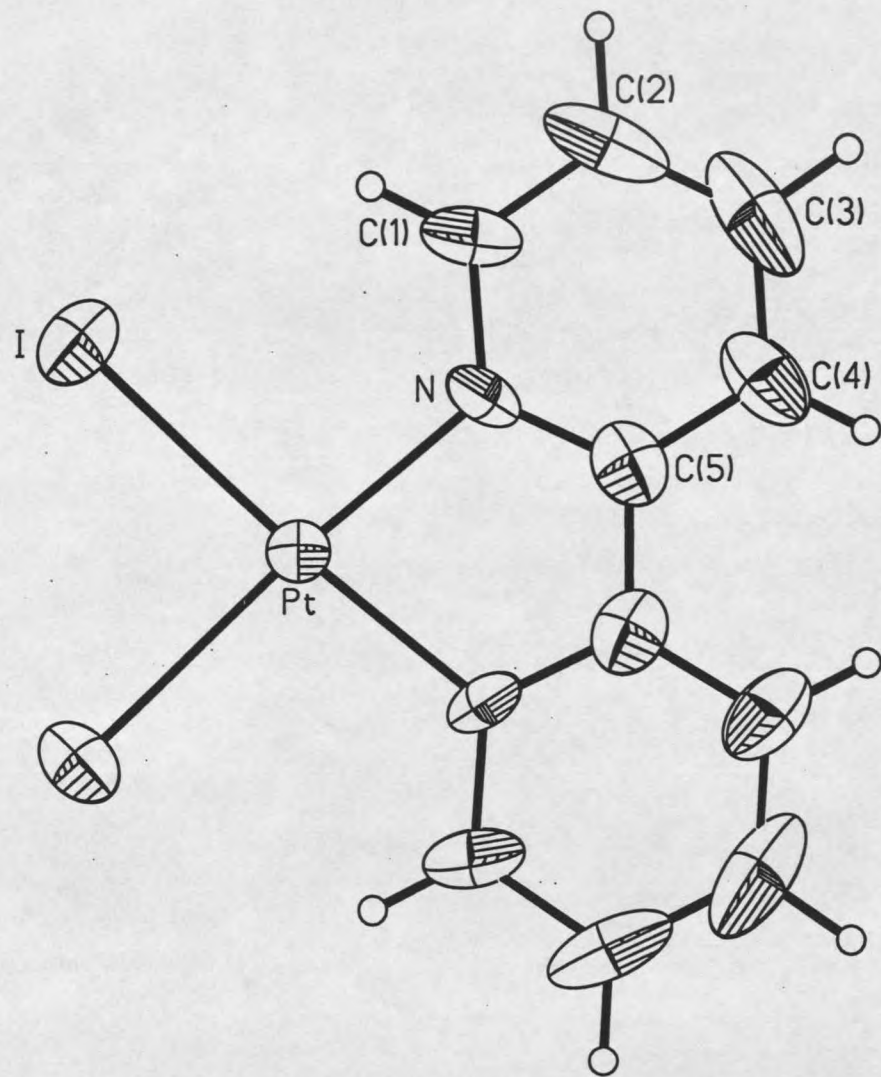


**Figure 4.** Thermal ellipsoid plot of 41 showing 50% probability ellipsoids and numbering scheme for the structure.

**Table 11.** Crystallographic data for Pt(bipy)Br<sub>2</sub> (**40**) and Pt(bipy)I<sub>2</sub> (**41**).

Parameter	<b>40</b>	<b>41</b>
Formula	C <sub>10</sub> H <sub>8</sub> N <sub>2</sub> Br <sub>2</sub> Pt	C <sub>10</sub> H <sub>8</sub> N <sub>2</sub> I <sub>2</sub> Pt
Formula weight	511.1	605.1
Space Group	C2/c	C2/c
Unit cell: a (Å)	17.262(5)	17.405(2)
b (Å)	9.388(2)	9.805(2)
c (Å)	7.557(2)	7.706(1)
β (°)	113.47(2)	112.09(1)
volume (Å <sup>3</sup> )	1123.5(5)	1208.5(4)
Z	4	4
ρ (g cm <sup>-3</sup> ) calculated	3.022	3.298
absorption coef, Mo K <sub>α</sub> (cm <sup>-1</sup> )	195.7	165.5
F(000)	920	1064

**Table 12.** Data collection and structure refinement data for **40** and **41**.

Parameter	<b>40</b>	<b>41</b>
2 $\theta$ range (°)	4-65	4-65
Unique reflections	1638	2203
Observed reflections	1126	1012
Number of parameters	69	69
Trans. Factor range	0.075-0.877	0.561-0.762
Final R <sup>a</sup> , observed data	0.049	0.057
Final wR <sup>b</sup> , observed data	0.048	0.025
Final wR <sup>b</sup> , all data	0.055	0.033
Goodness of fit	1.02	1.21
<sup>a</sup> $R = \sum    F_o  -  F_c    / \sum  F_o $ . <sup>b</sup> $wR = [\sum(w(F_o^2 - F_c^2)^2) / \sum wF_o^4]^{1/2}$ where $w = [\sigma^2(F) + 0.0007F^2]^{-1}$		

**Table 13.** Atomic Coordinates and equivalent isotropic displacement coefficients for 40.

Atoms	x/a	y/b	z/c	U(eq)
Pt	0.00000	0.30922(6)	0.25000	0.0327(2)
Br	-0.0991(1)	0.1252(1)	0.0753(2)	0.0640(6)
N	-0.0762(6)	0.4731(9)	0.118(1)	0.033(3)
C(1)	-0.1561(7)	0.463(1)	-0.025(2)	0.045(5)
C(2)	-0.20(1)	0.584(2)	-0.107(2)	0.073(7)
C(3)	-0.1670(9)	0.715(1)	-0.053(2)	0.063(7)
C(4)	-0.0883(8)	0.725(1)	0.087(2)	0.052(6)
C(5)	-0.0425(7)	0.605(1)	0.174(2)	0.037(4)

**Table 14.** Bond lengths (Å) for **40**.

Bond	Length(Å)	Bond	Length(Å)
Pt-Br	2.420(2)	Pt-N	2.010(8)
Pt-Br(A)	2.420(2)	Pt-N(A)	2.010(8)
N-C(1)	1.37(1)	N-C(5)	1.36(1)
C(1)-C(2)	1.37(2)	C(2)-C(3)	1.35(2)
C(3)-C(4)	1.35(2)	C(4)-C(5)	1.39(1)
C(5)-C(5A)	1.46(2)		

**Table 15.** Bond angles (°) for **40**.

Atoms	Angles(°)	Atoms	Angles(°)
Br-Pt-N	95.5(2)	Br-Pt-Br(A)	88.9(1)
N-Pt-Br(A)	175.6(2)	Br-Pt-N(A)	175.6(2)
N-Pt-N(A)	80.1(4)	Br(A)-Pt-N(A)	95.5(2)
Pt-N-C(1)	126.1(7)	Pt-N-C(5)	115.4(6)
C(1)-N-C(5)	118.4(9)	N-C(1)-C(2)	121(1)
C(1)-C(2)-C(3)	121(1)	C(2)-C(3)-C(4)	119(1)
C(3)-C(4)-C(5)	121(1)	N-C(5)-C(4)	120(1)
N-C(5)-C(5A)	114.5(5)	C(4)-C(5)-C(5A)	125.2(6)

**Table 16.** Anisotropic displacement coefficients for **40**.

Atom	$U_{xx}$	$U_{yy}$	$U_{zz}$	$U_{xy}$	$U_{xz}$	$U_{yz}$
Pt	0.0360(3)	0.0239(3)	0.0308(3)	0.0000	0.0057(2)	0.0000
Br	0.067(1)	0.0362(7)	0.0641(9)	-0.0134(6)	0.0006(8)	-0.0111(6)
N	0.029(5)	0.035(5)	0.035(5)	0.008(4)	0.012(4)	0.004(4)
C(1)	0.0360(6)	0.053(7)	0.037(6)	-0.001(5)	0.005(5)	0.003(5)
C(2)	0.060(9)	0.08(1)	0.059(9)	0.031(9)	0.005(8)	0.0113(8)
C(3)	0.070(9)	0.051(9)	0.08(1)	0.034(7)	0.038(8)	0.033(7)
C(4)	0.048(7)	0.026(6)	0.079(9)	0.012(5)	0.023(7)	0.012(5)
C(5)	0.038(7)	0.028(5)	0.044(7)	0.001(5)	0.014(5)	-0.0001(5)

The anisotropic displacement exponent takes the form:  $-2\pi^2(h^2a^2U_{xx} + \dots + 2hka^*b^*U_{xy})$

**Table 17.** Atomic Coordinates and equivalent isotropic displacement coefficients for 41.

Atoms	x/a	y/b	z/c	U(eq)
Pt	0.00000	0.31495(7)	0.25000	0.0341(3)
I	-0.10137(6)	0.12497(9)	0.0691(1)	0.0668(5)
N	-0.0743(5)	0.476(1)	0.121(1)	0.039(4)
C(1)	-0.1506(6)	0.464(1)	-0.013(2)	0.053(6)
C(2)	-0.1941(9)	0.584(2)	-0.090(2)	0.074(7)
C(3)	-0.159(1)	0.712(2)	-0.032(2)	0.083(9)
C(4)	-0.0806(8)	0.721(1)	0.106(2)	0.059(7)
C(5)	-0.0411(7)	0.6021(1)	0.179(2)	0.045(6)



**Table 18.** Bond lengths (Å) for **41**.

Bond	Length(Å)	Bond	Length(Å)
Pt-I	2.584(1)	Pt-N	2.045(9)
Pt-I(A)	2.584(1)	Pt-N(A)	2.045(9)
N-C(1)	1.35(1)	N-C(5)	1.37(2)
C(1)-C(2)	1.39(2)	C(2)-C(3)	1.40(2)
C(3)-C(4)	1.38(2)	C(4)-C(5)	1.36(2)
C(5)-C(5A)	1.43(2)		

**Table 19.** Bond angles (°) for **41**.

Atoms	Angles(°)	Atoms	Angles(°)
I-Pt-N	96.6(2)	I-Pt-I(A)	87.7(1)
N-Pt-I(A)	175.7(2)	I-Pt-N(A)	175.7(2)
N-Pt-N(A)	79.2(5)	I(A)-Pt-N(A)	96.6(2)
Pt-N-C(1)	125.4(8)	Pt-N-C(5)	115.2(6)
C(1)-N-C(5)	119(1)	N-C(1)-C(2)	119(1)
C(1)-C(2)-C(3)	121(1)	C(2)-C(3)-C(4)	119(1)
C(3)-C(4)-C(5)	118(1)	N-C(5)-C(4)	123(1)
N-C(5)-C(5A)	115.2(5)	C(4)-C(5)-C(5A)	121.4(7)

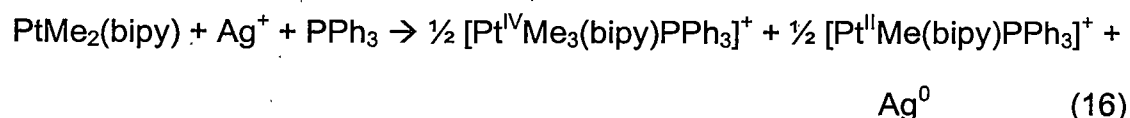
**Table 20.** Anisotropic displacement coefficients ( $\text{\AA}^2$ ) for **41**.

Atom	$U_{xx}$	$U_{yy}$	$U_{zz}$	$U_{xy}$	$U_{xz}$	$U_{yz}$
Pt	0.0331(4)	0.0306(4)	0.0335(4)	0.0000	0.0068(3)	0.0000
I	0.0654(7)	0.0491(7)	0.0674(7)	-0.0148(5)	0.0038(5)	-0.0105(5)
N	0.031(6)	0.042(7)	0.036(5)	0.014(5)	0.005(5)	0.01(5)
C(1)	0.027(7)	0.08(1)	0.046(7)	-0.010(7)	0.005(5)	0.004(8)
C(2)	0.050(9)	0.12(1)	0.044(8)	0.04(1)	0.011(7)	0.03(1)
C(3)	0.09(1)	0.07(1)	0.12(1)	0.04(1)	0.07(1)	0.05(1)
C(4)	0.050(9)	0.06(1)	0.07(1)	0.024(8)	0.031(8)	0.021(8)
C(5)	0.047(8)	0.043(8)	0.054(9)	0.007(7)	0.028(7)	0.008(7)

The anisotropic displacement exponent takes the form:  $-2\pi^2(h^2a^2U_{xx} + \dots + 2hka^*b^*U_{xy})$

Preparation of the Dimeric Pt(III) Complexes

In 1988, Puddephatt et al. discussed the reaction between PtMe<sub>2</sub>(bipy) (33) and silver(I) in acetone as shown in Equation 16 (79):



At first glance, this reaction appears to be very straightforward. One mole of PtMe<sub>2</sub>(bipy) reacted with one mole of silver(I) to produce equimolar amounts of the *fac*-Pt<sup>IV</sup>Me<sub>3</sub> and Pt<sup>II</sup>Me complexes. He explained Equation 16 as "the oxidation of Pt(II) to Pt(IV), with transfer of a methyl group from a further molecule of PtMe<sub>2</sub>(bipy) to Pt(IV)...and this...leads to equimolar amount of *fac*-Pt<sup>IV</sup>Me<sub>3</sub> and Pt<sup>II</sup>Me units. The mechanism of reaction is unknown (79)." At the time that this work was published, very little was known about dimeric Pt(III) chemistry. However, with today's knowledge of Pt(III) chemistry, one realizes that the products in Equation 16 do not form as Puddephatt described.

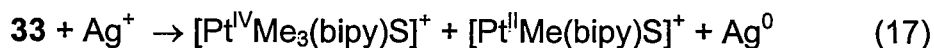
Experiments were run with two or more mole equivalents of Ag(I) added to PtMe<sub>2</sub>(diimine) solutions. The results showed that Ag(I) is not capable of completely oxidizing Pt<sup>II</sup>Me<sub>2</sub>(diimine) to a Pt(IV) complex, either [Pt<sup>IV</sup>Me<sub>3</sub>(diimine)X]<sup>+</sup> or [Pt<sup>IV</sup>Me<sub>2</sub>(diimine)X<sub>2</sub>]<sup>2+</sup>. However, the same products as shown in Equation 16 were obtained. Consequently, Puddephatt could not have formed the products in the manner that he described. However, it is known that

when a dimeric Pt(III) complex disproportionates, the products that are produced are equimolar amounts of Pt(IV) and Pt(II). Therefore, the mechanism through which Equation 16 proceeded was most likely through a dimeric Pt(III) complex and the methyl transfer also occurred through the dimeric Pt(III) complex.

Even with the extensive  $^1\text{H}$  NMR studies that Puddephatt et al. performed, working at temperatures as low as 183 K, he did not observe an intermediate dimeric Pt(III) species. Therefore, the existence of the dimeric Pt(III) species must have been extremely short-lived with his reaction conditions; however, it must be present and my goal was to isolate this species.

Preparation of the dimeric Pt(III) species: **36** and **37**.

Puddephatt et al. had run their reactions in the presence of triphenylphosphine ( $\text{PPh}_3$ ) and in acetone. My initial intention was to study what would happen in acetonitrile. Although acetonitrile is a suitable ligand for platinum, it is much less so than acetone. When one equivalent of silver(I) was reacted with  $\text{PtMe}_2(\text{diimine})$ , where diimine = bipy or phen, in acetonitrile, the following products were obtained (Figure 5 for **33** and Figure 6 for **34**) as shown by Equation 17.



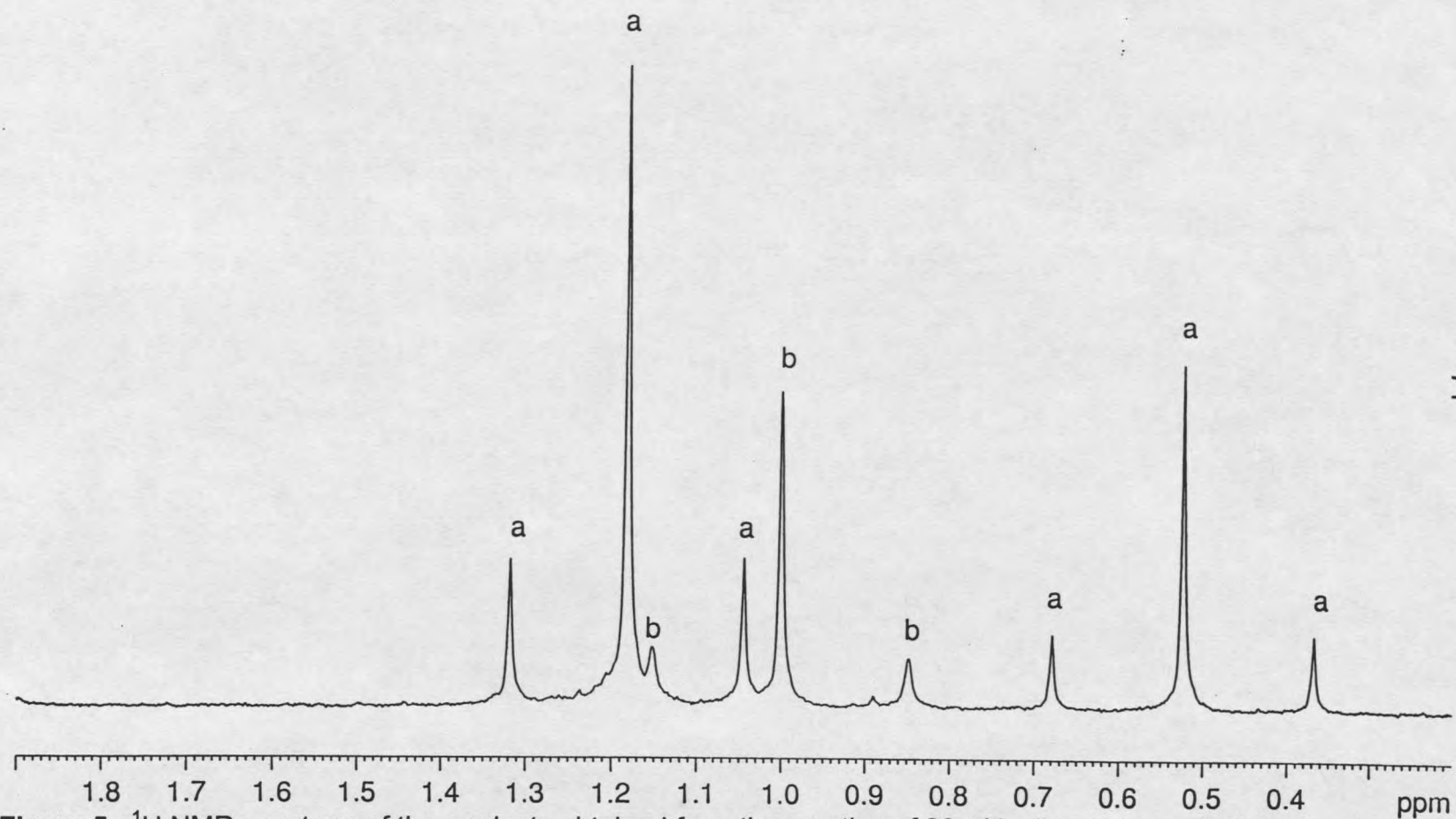


**Figure 5.**  $^1\text{H}$  NMR spectrum of the products obtained from the reaction of **33** with silver(I) in acetonitrile- $\text{d}_3$ . Peak labels are (a)  $\text{fac-}[\text{Pt}^{\text{IV}}\text{Me}_3(\text{bipy})\text{S}]^+$  and (b)  $[\text{Pt}^{\text{II}}\text{Me}(\text{bipy})\text{S}]^+$ , where S = solvent.























































































































































































































































































